© 2022. Published by The Company of Biologists Ltd | Journal of Cell Science (2022) 135, jcs258584. doi:10.1242/jcs.258584

RESEARCH ARTICLE

Phospholipase C-related but catalytically inactive protein acts as a positive regulator of insulin signalling in adipocytes

Jing Gao[1,*], Akiko Mizokami[2], Hiroshi Takeuchi[3], Aonan Li[1], Fei Huang[1], Haruki Nagano[1], Takashi Kanematsu[4], Eijiro Jimi[1,2] and Masato Hirata[5,*]

ABSTRACT

Insulin signalling is tightly controlled by various factors, but the exact molecular mechanism remains incompletely understood. We have previously reported that phospholipase C-related but catalytically inactive protein (PRIP; used here to refer to both PRIP-1 and PRIP-2, also known as PLCL1 and PLCL2, respectively) interacts with Akt1, the central molecule in insulin signalling. Here, we investigated whether PRIP is involved in the regulation of insulin signalling in adipocytes. We found that insulin signalling, including insulin-stimulated phosphorylation of the insulin receptor (IR), insulin receptor substrate-1 (IRS-1) and Akt, and glucose uptake were impaired in adipocytes from PRIP double-knockout (PRIP-KO) mice compared with those from wild-type (WT) mice. The amount of IR expressed on the cell surface was decreased in PRIP-KO adipocytes. Immunoprecipitation assays showed that PRIP interacted with IR. The reduced cell surface IR in PRIP-KO adipocytes was comparable with that in WT cells when Rab5 (Rab5a, -5b and -5c) expression was silenced using specific siRNA. In contrast, the dephosphorylation of IRS-1 at serine residues, some of which have been reported to be involved in the internalisation of IR, was impaired in cells from PRIP-KO mice. These results suggest that PRIP facilitates insulin signalling by modulating the internalisation of IR in adipocytes.

KEY WORDS: Insulin signalling, Insulin receptor, Insulin receptor substrate-1, Adipocyte, Insulin resistance

INTRODUCTION

The prevalence of obesity and obesity-associated disorders, including metabolic syndrome and type 2 diabetes, is predicted to continue being a health hazard over the coming decades. The principal feature of these modern-world diseases is insulin resistance, which is characterised by compromised responsiveness to normal insulin levels. Thus, understanding the molecular mechanisms underlying insulin resistance has become increasingly important for the development of future therapies.

[1]Laboratory of Molecular and Cellular Biochemistry, Faculty of Dental Science, Kyushu University, 3-1-1 Maidashi, Higashi-ku, Fukuoka 812-8582, Japan. [2]Oral Health/Brain Health/Total Health Research Center, Faculty of Dental Science, Kyushu University, 3-1-1 Maidashi, Higashi-ku, Fukuoka 812-8582, Japan. [3]Division of Applied Pharmacology, Kyushu Dental University, 2-6-1 Manazuru, Kokurakita-ku, Kitakyushu 803-8580, Japan. [4]Department of Cell Biology and Pharmacology, Faculty of Dental Science, Kyushu University, 3-1-1 Maidashi, Higashi-ku, Fukuoka 812-8582, Japan. [5]Oral Medicine Research Center, Fukuoka Dental College, 2-15-1 Tamura, Sawara-ku, Fukuoka 814-0193, Japan.

*Authors for correspondence (orchid@dent.kyushu-u.ac.jp; hirata@college.fdcnet.ac.jp)

J.G., 0000-0002-1568-0665

Handling Editor: John Heath
Received 2 March 2021; Accepted 15 November 2021

Binding of insulin to the insulin receptor (IR) activates its intrinsic tyrosine kinase, which undergoes autophosphorylation, leading to the activation of the insulin signalling cascade (Lemmon and Schlessinger, 2010). Insulin signalling is mediated by a complicated network of a variety of effector proteins, whose perturbations can manifest as insulin resistance (Boucher et al., 2014). The mature form of IR, a tetrameric plasma membrane protein consisting of a dimer of two disulfide-linked chains, IRα and IRβ, is a dynamic molecule that is transported through multiple cellular compartments and undergoes constitutive endocytosis at the cell surface (Goh and Sorkin, 2013; Knutson, 1991). The appropriate amount of IR in the plasma membrane is determined by the balance between trafficking to the plasma membrane and endocytosis of IR, which allows maximal access to the extracellular ligand, insulin. Any interference in the maintenance of IR in the plasma membrane can impair insulin signalling (Starks et al., 2015; Choi et al., 2016); however, the molecular mechanisms underlying IR trafficking and internalisation from the plasma membrane are not yet completely understood.

Impaired insulin signalling by the phosphorylation of insulin receptor substrate-1 (IRS-1) and IRS-2 on serine and threonine residues has been reported to be the principal molecular mechanism of insulin resistance (Copps and White, 2012; Boucher et al., 2014; Samuel and Gerald, 2012). Several different mechanisms, including altered interactions with IR (Paz et al., 1997; Kim et al., 2005; Nawaratne et al., 2006), altered internalisation of IR (Choi et al., 2019), and changes to the intracellular localisation of IRS-1 and its eventual degradation (Harrington et al., 2004; Shah et al., 2004; Yoneyama et al., 2018a), are thought to be involved, although the precise underlying mechanism is poorly understood.

Phospholipase C-related but catalytically inactive protein (PRIP) – which has two forms, PRIP-1 and PRIP-2 (also known as PLCL1 and PLCL2, respectively) – was originally identified as a D-*myo*-inositol 1,4,5-trisphosphate [Ins(1,4,5)P_3]-binding protein (Kanematsu et al., 1992). Previous studies have revealed that PRIP functions as a scaffold protein and has many binding partners, including the protein phosphatase 1 α catalytic subunit (PP1α, also known as PPP1CA) (Yoshimura et al., 2001; Gao et al., 2012), protein phosphatase 2A (PP2A) (Sugiyama et al., 2012, 2013), the β subunit of the $GABA_A$ receptor (Terunuma et al., 2004; Kanematsu et al., 2006), SNARE proteins (Gao et al., 2012; Zhang et al., 2013) and the phosphorylated form of Akt1 (Fujii et al., 2010), in addition to Ins(1,4,5)P_3 and phosphatidylinositol 4,5-bisphosphate [PtdIns(4,5)P_2] (Takeuchi et al., 1996, 2000; Harada et al., 2005; Gao et al., 2009; Kanematsu et al., 2002; Asano et al., 2017). PRIP mediates several biological functions, including Ins(1,4,5)P_3–Ca^{2+} signalling, $GABA_A$ receptor signalling, dephosphorylation of proteins and exocytosis, by interacting with these molecules.

We have previously reported that PRIP-1 and PRIP-2 double-knockout (PRIP-KO) mice exhibit a lean phenotype with less

Journal of Cell Science (2022) 135, jcs258584. doi:10.1242/jcs.258584

white adipose tissue (WAT) mass due to enhanced lipolysis (Okumura et al., 2014). As PRIP interacts with active Akt and protein phosphatases, we speculated that it might also be involved in the regulation of insulin signalling. In the present study, we examined insulin signalling in the adipocytes and adipose tissue of PRIP-KO mice and compared it to that in wild-type (WT) mice. The results suggest that ablation of PRIP diminishes the plasma membrane localisation of IR by promoting its internalisation, impairing insulin signalling in adipocytes.

RESULTS

Deficiency of PRIP causes impaired insulin signalling

To verify our hypothesis that PRIP might be involved in the regulation of insulin signalling, we firstly examined the phosphorylation of IR and Akt in WAT dissected from WT and PRIP-KO mice 5 min after intraperitoneal injection of insulin (0.025 U/kg). Increased phosphorylation of IR at tyrosine 1361 and of Akt at threonine 308 was observed in WAT from insulin-injected WT mice, but this was diminished in WAT from PRIP-KO mice (Fig. 1A).

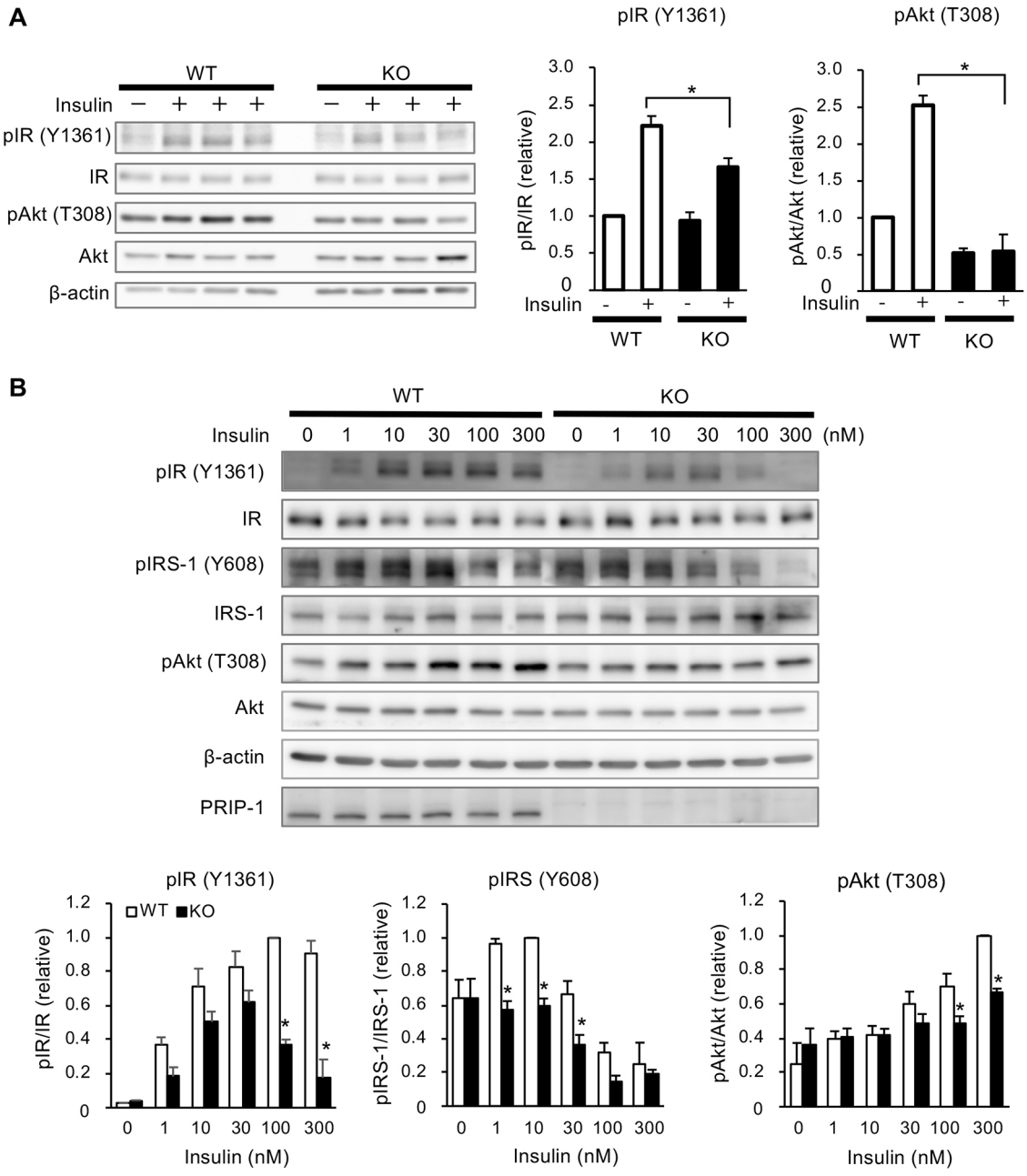

Fig. 1. Insulin signalling is impaired in adipocytes from PRIP-KO mice. (A) WT and PRIP-KO male mice were intraperitoneally injected with human insulin (0.025 U/kg). Perigonadal WAT was isolated 5 min after the injection and snap-frozen in liquid nitrogen. The extracted tissue lysates were prepared, and 10 µg of protein from each sample was used for SDS–PAGE and analysed by western blotting to detect the indicated proteins and phosphorylated proteins. (B) MEF cells isolated from WT and PRIP-KO mice were cultured in a 12-well plate and differentiated to adipocytes (MEF-derived adipocytes). After starvation in a serum-free medium for 12–16 h, cells were stimulated with insulin at the indicated concentrations for 5 min. Extracted proteins in the cell lysates were analysed by SDS–PAGE and western blotting to detect the indicated proteins and phosphoproteins. Representative blots and quantitative data are shown in A and B. β-actin is shown as a loading control. Data are the mean±s.e.m. from four independent experiments. *P<0.05, versus the corresponding WT value (Mann–Whitney test).

Journal of Cell Science (2022) 135, jcs258584. doi:10.1242/jcs.258584

To confirm the effect of PRIP deficiency on insulin signalling in adipocytes, we prepared adipocytes differentiated from mouse embryonic fibroblast (MEF) cells derived from the embryos of WT and PRIP-KO mice (MEF-derived adipocytes). Assessment using Oil Red O staining and immunoblotting analysis of adipogenic markers, including adiponectin and peroxisome proliferator-activated receptor γ (PPAR γ), revealed that these cells from the WT and PRIP-KO mice show a similar degree of adipocyte differentiation (Fig. S1A,B). The expression of GLUT4 (also known as SLC2A4) in MEF-derived adipocytes from WT and PRIP-KO mice was also determined to be analogous (Fig. S1A). Moreover, stimulation of these adipocytes with insulin revealed results comparable to those observed in the *in vivo* experiment (Fig. 1A). Insulin stimulation for 5 min triggered the phosphorylation of IR at tyrosine 1361 and of Akt at threonine 308 in a dose-dependent manner, indicating activation of insulin signalling in WT MEF-derived adipocytes, and we observed diminished activation in PRIP-KO MEF-derived adipocytes (Fig. 1B). The phosphorylation of IRS-1 at tyrosine 608 in WT adipocytes was triggered by insulin up to 10 nM but was attenuated by insulin concentrations greater than 30 nM. In contrast, there were low phosphorylation levels in PRIP-KO adipocytes (Fig. 1B). We also obtained results similar to those observed for MEF-derived adipocytes in experiments using primary cultured WAT dissected from WT and PRIP-KO mice (Fig. S1C).

The reduction of insulin signalling in adipocytes from PRIP-KO mice was confirmed by monitoring the cell surface translocation of GLUT4 and glucose uptake, a major cellular function mediated by insulin signalling in adipocytes. Insulin induces the translocation of GLUT4 to the plasma membrane of adipocytes through the activation of Akt, resulting in enhanced glucose uptake. We differentiated 3T3-L1 cells into adipocytes and transiently transfected them with a construct for expression of HA-tagged GLUT4–GFP. This construct was designed to facilitate evaluation of the plasma membrane localisation of GLUT4 using an anti-HA antibody to detect an HA epitope located in the first extracellular loop. Our results showed that in non-permeabilised cells, anti-HA signals were evident in the control scrambled siRNA-transfected cells after insulin stimulation (Fig. 2A,B); however, insulin-triggered GLUT4 translocation was practically abrogated in cells transfected with siRNAs targeting PRIP-1 and PRIP-2. Furthermore, glucose uptake upon insulin stimulation was diminished in adipocytes from PRIP-KO MEF-derived adipocytes (Fig. 2C). The same result was observed in *ex vivo* organ cultures of WAT prepared from WT and PRIP-KO mice (Fig. 2D), indicating that insulin signalling is functionally impaired by the deletion of PRIP in adipocytes.

PRIP inhibits constitutive endocytosis of IR

The reduction in insulin-stimulated IR phosphorylation in the absence of PRIP indicates that PRIP acts upstream in the insulin signalling pathway, possibly at the level of IR itself in terms of quality or quantity. We speculated that because maximal access of insulin to IR depends on the amount of IR on the plasma membrane of adipocytes, this could be reduced by PRIP deficiency. To examine the cell surface expression of IR, we performed a cell surface biotinylation assay in which plasma membrane proteins were biotinylated, followed by precipitation of biotin-associated proteins. The level of IR in the plasma membrane of adipocytes derived from MEFs of KO mice was reduced by ∼25% compared with the level in MEF-derived adipocytes from WT mice, although the total IR, including that in intracellular compartments, was unchanged (Fig. 3A).

To explore the mechanisms related to the reduction of IR on the plasma membrane upon deletion of PRIP, we performed a biotinylation assay to investigate the internalisation of IR. Cell surface proteins were biotinylated with sulfo-NHS-SS-biotin, followed by incubation at 37°C for 20 min to induce constitutive internalisation without any stimulation. Cells were then treated with glutathione to remove biotin, so that only the proteins that were internalised into the cells remained biotinylated. Our results revealed that incubation for 20 min triggered the internalisation of cell surface IR into adipocytes. Furthermore, the amount of internalised IR in PRIP-KO MEF-derived adipocytes was ∼30% higher than that in WT MEF-derived adipocytes (Fig. 3B), indicating that the internalisation of IR was upregulated by deletion of PRIP in adipocytes.

Receptors in the plasma membrane undergo clathrin-dependent endocytosis into Rab5-positive early endosomes followed by recycling back to the cell surface or transportation to late endosomes that fuse to lysosomes for degradation (Goh and Sorkin, 2013; Zerial and McBride, 2001; Su et al., 2006). We examined the amount of IR in the plasma membrane of adipocytes derived from MEF cells after transfection with siRNAs targeting Rab5a, Rab5b and Rab5c. A decrease of IR on the plasma membrane of PRIP-KO adipocytes was not observed when the expression of Rab5 was downregulated using siRNA, whereas decreased IR was observed on the plasma membrane of adipocytes from PRIP-KO MEFs treated with control scrambled siRNA (Fig. 3A,C). Furthermore, treatment of WT MEF-derived adipocytes with primaquine, an inhibitor of recycling (van Weert et al., 2000), reduced the levels of IR on the cell surface, indicating that the endocytosis recycling process is involved in the maintenance of IR levels on the plasma membrane (Fig. 3D). This reduction of IR on the cell surface by primaquine was also observed in PRIP-KO MEF-derived adipocytes, suggesting that PRIP is not involved in the recycling process. Taken together, these results suggest that PRIP deficiency promotes constitutive endocytosis.

Next, we examined the subcellular localisation of PRIP-1 and IR, considering the close association between them. We co-transfected 3T3-L1 adipocytes with vectors encoding GFP-tagged IR and either DsRed-tagged PRIP-1 or DsRed alone as a control. Cells were stimulated with insulin for 15 min before fixation in 4% paraformaldehyde (PFA), followed by immunocytochemistry. As shown in Fig. 4A, GFP–IR was predominantly localised in the plasma membrane, and upon insulin stimulation of control (empty DsRed vector-transfected) cells, the levels of plasma membrane-localised IR diminished and GFP–IR was internalised into intracellular compartments. However, in DsRed–PRIP-1-expressing cells, PRIP-1 colocalised with GFP–IR before insulin stimulation, and GFP–IR remained on the plasma membrane even after insulin stimulation. We assumed that PRIP interacted with IR in the cytosol to prevent endocytosis. To examine this possibility, we used HepG2 cells, which do not express detectable levels of PRIP-1, instead of 3T3-L1 cells due to the low transfection efficiency of plasmid DNA. We performed a co-immunoprecipitation assay using HepG2 cells stably overexpressing GFP tagged PRIP-1. GFP–PRIP-1 was immunoprecipitated from cell lysates using a specific antibody against GFP, followed by western blotting with an anti-IR antibody. IR was co-immunoprecipitated with GFP–PRIP-1 but not with GFP alone (Fig. 4B), indicating that PRIP-1 interacts with IR, which might prevent constitutive endocytosis.

PRIP deficiency enhances the serine phosphorylation of IRS-1

Although the molecular mechanism by which the internalisation of IR is regulated has not been fully elucidated, it has recently been

Journal of Cell Science (2022) 135, jcs258584. doi:10.1242/jcs.258584

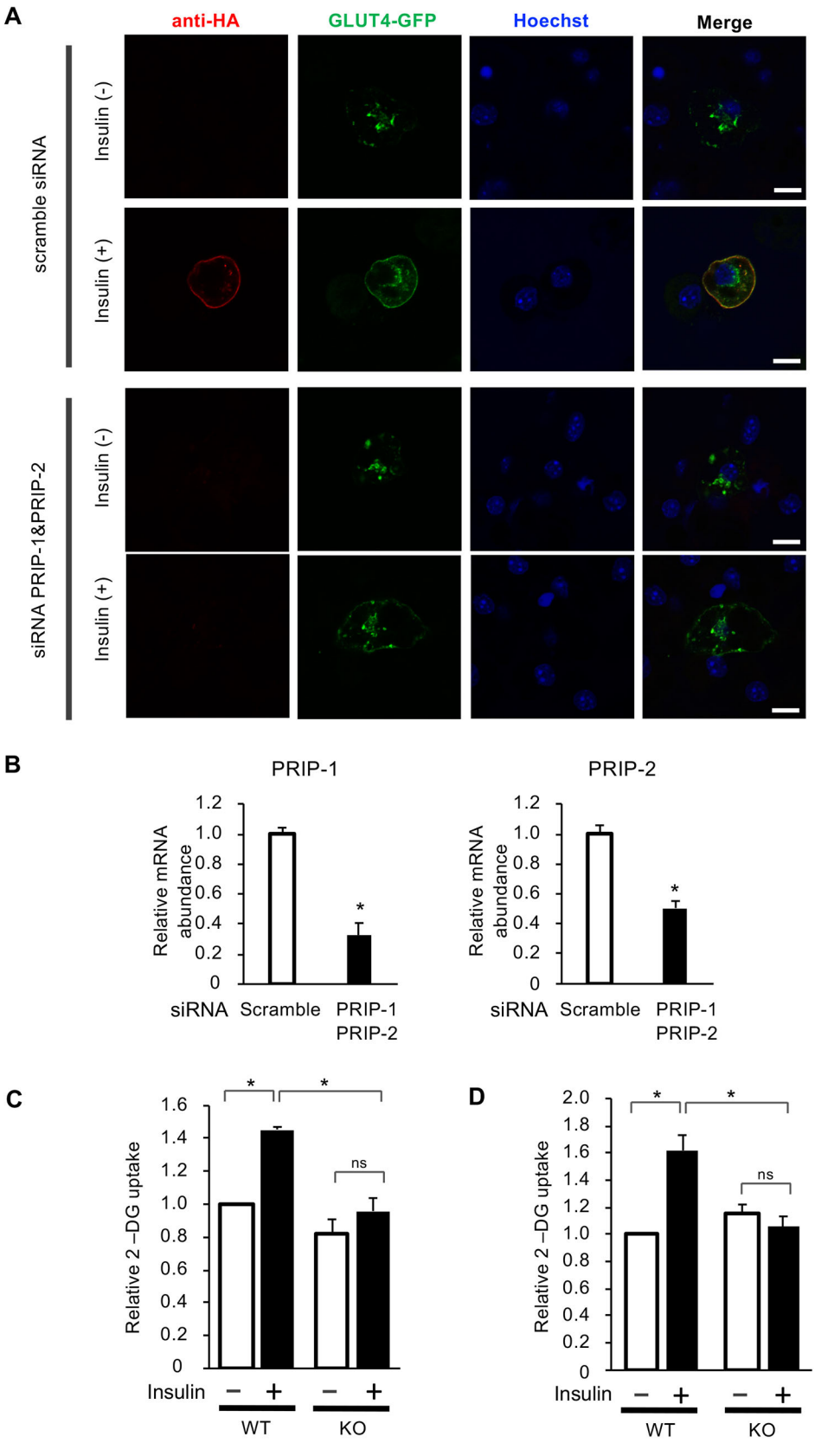

Fig. 2. Insulin-induced GLUT4 translocation and glucose uptake is impaired in adipocytes from PRIP-KO mice. (A) 3T3-L1 cells were cultured on coverslips in a 24-well plate and differentiated into adipocytes. The differentiated adipocytes were co-transfected with a construct expressing HA-tagged GLUT4–GFP and either control scramble siRNA or siRNAs against PRIP-1 and PRIP-2. Cells were stimulated with 20 nM insulin for 15 min after 6 h of serum starvation, followed by fixation without permeabilisation. Exofacial HA exposure on the outer membrane of the cells was visualised by immunostaining using an anti-HA antibody followed by the incubation of cells with Alexa Fluor 594-conjugated goat secondary antibodies. Nuclei were stained using Hoechst 33258. Representative images of GLUT4 translocation are shown, from a total of four experiments. Scale bars: 10 µm. (B) Quantitative RT-PCR analysis of relative mRNA abundance for *Prip-1* and *Prip-2* in 3T3L1 adipocytes transfected with siRNA as described in A. Results were normalised by the amount of *Gapdh* mRNA. Data are mean±s.e.m. from four independent experiments. **P*<0.05, versus the scramble siRNA-transfected cells (Mann–Whitney test). (C) Glucose (2-DG) uptake in WT and PRIP-KO MEF-derived adipocytes was measured after stimulation with 20 nM insulin or vehicle for 20 min. (D) Perigonadal WAT (pgWAT) was isolated from WT and PRIP-KO mice. The pgWAT was cut into small pieces and cultured in serum-free M199 medium for 16 h. Then, glucose (2-DG) uptake in *ex vivo* adipose tissue was measured after stimulation with 20 nM insulin or vehicle for 20 min. Data in C and D are the mean±s.e.m. from four independent experiments, normalised to the vehicle-treated WT sample. **P*<0.05; ns, not significant (Mann–Whitney test).

reported that phosphorylation of IRS-1 at serine 612 by extracellular signal-regulated kinase 1 and 2 (ERK1/2; also known as MAPK3 and MAPK1, respectively) promotes the endocytosis of IR (Choi et al., 2019). To investigate the relationship between the serine/threonine phosphorylation of IRS-1 and the amount of cell surface IR, we treated adipocytes differentiated from 3T3-L1 cells with phorbol 12-myristate 13-acetate (PMA) for 30 min to activate protein kinase C and experimentally phosphorylate IRS-1. PMA

Journal of Cell Science (2022) 135, jcs258584. doi:10.1242/jcs.258584

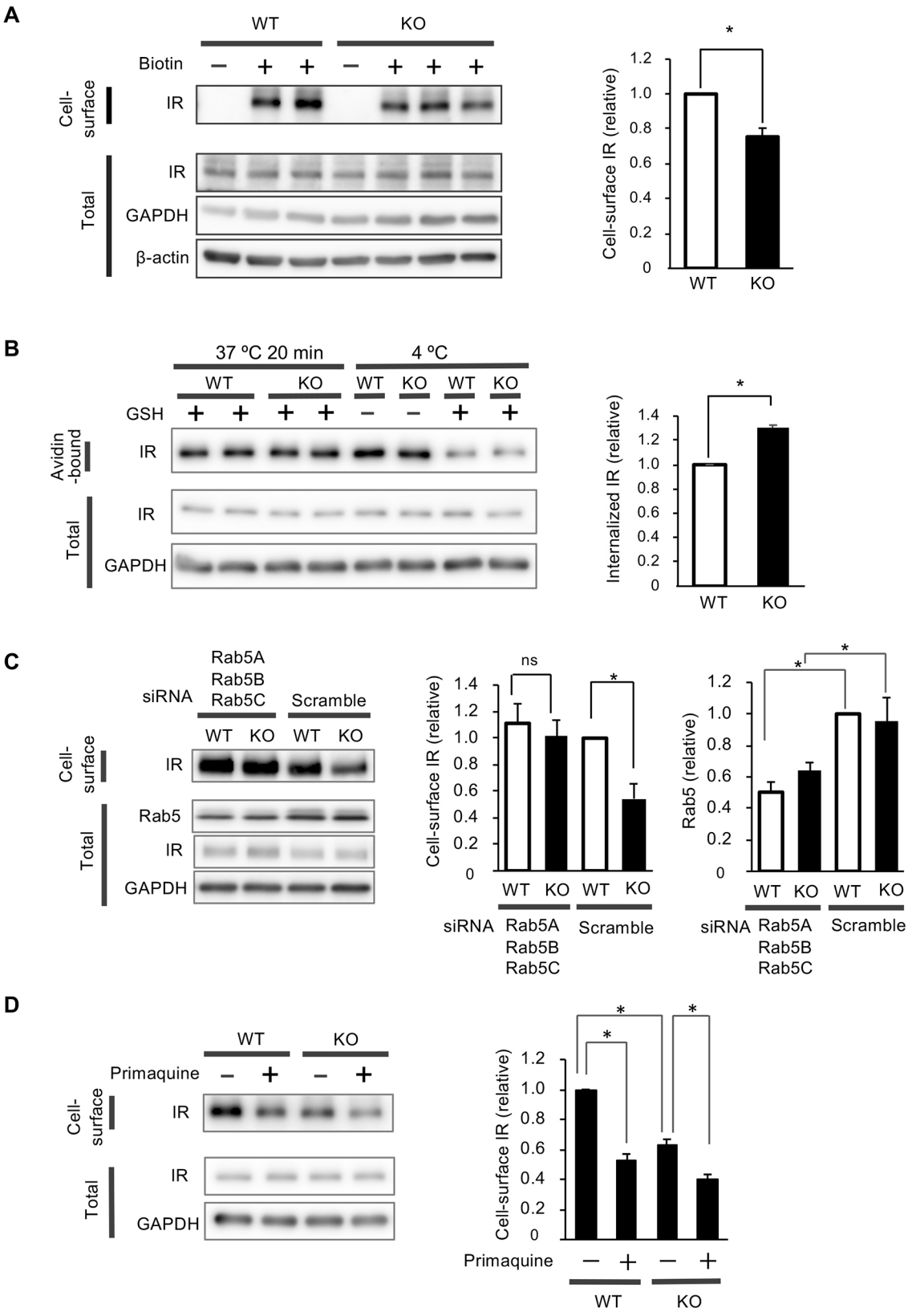

Fig. 3. See next page for legend.

treatment induced a robust phosphorylation of IRS-1 at serine 612, as well as at serine 632 and serine 1097, both of which are substrates of mTORC1 (Tzatsos and Kandror, 2006; Tzatsos, 2009) and p70S6K (Zhang et al., 2008; Tremblay et al., 2007), which function downstream of the IR–IRS-1–Akt cascade. The amount of IR localised on the plasma membrane was markedly reduced, as assessed using a cell surface biotinylation assay (Fig. 5). These results suggest that the phosphorylation of serine residues in IRS-1,

Journal of Cell Science (2022) 135, jcs258584. doi:10.1242/jcs.258584

Fig. 3. Internalisation of IR on plasma membranes is enhanced in adipocytes from PRIP-KO mice. (A) MEF cells isolated from WT and PRIP-KO mice were cultured in 6-well plates and differentiated to adipocytes. A cell surface biotinylation assay was performed using sulfo-NHS-LC-biotin. Biotinylated cell surface proteins associated with NeutraAvidin beads and total cell lysates were subjected to SDS–PAGE and western blotting to detect the indicated proteins. (B) WT and PRIP-KO MEF cells were cultured and differentiated into adipocytes as described in A. After labelling cell surface proteins with sulfo-NHS-SS-biotin at 4°C, cells were incubated at 37°C for 20 min. After treatment with reduced glutathione (GSH), the remaining biotinylated proteins were precipitated using NeutraAvidin beads, followed by separation with SDS–PAGE and analysis by western blotting. Internalised IR was assessed by calculating the ratio of biotinylated IR from cells incubated at 37°C, after subtracting the value of biotinylated IR with glutathione treatment at 4°C, to that from cells incubated at 4°C without glutathione treatment. (C) WT and PRIP-KO MEF-derived adipocytes were transfected with control scrambled siRNA or mixed siRNAs against individual Rab5 isoforms (Rab5A, B and C). After 48 h, a biotinylation assay was performed as described in A. (D) WT and PRIP-KO MEF-derived adipocytes were pretreated with 0.1 mM primaquine for 30 min before performing a cell surface biotinylation assay as described in A. In A–D, representative blots and quantitative data are shown. Data are the mean±s.e.m. from four independent experiments. **P*<0.05; ns, not significant (Mann–Whitney test).

including serine 612, might be involved in regulation of the endocytosis of IR.

We have previously reported that PRIP is involved in the regulation of dephosphorylation of proteins such as synaptosomal-associated protein of 25 kDa (SNAP-25) (Gao et al., 2012; Zhang et al., 2013) by recruiting PP1 and PP2A. Because the endocytosis of IR in PRIP-KO adipocytes might be promoted as mentioned above, we speculated that PRIP might be involved in regulation of the serine/threonine phosphorylation of IRS-1. We examined the insulin-induced phosphorylation of IRS-1 at serine residues 612, 632 and 1097 in MEF cells from WT or PRIP-KO mice. As shown in Fig. 6A, insulin induced the phosphorylation of IRS-1 at serine 612, serine 632, and serine 1097 in WT MEF cells in a dose-dependent manner, which was augmented in PRIP-KO MEF cells. Similar results were obtained when cells were treated with PMA (Fig. S2A). To determine whether the enhanced serine phosphorylation of IRS-1 was caused by reduced phosphatase-mediated dephosphorylation, we used an inhibitor of PP1 and PP2A, calyculin A. MEF cells from WT and PRIP-KO mice were pretreated with calyculin A at 0, 10 or 20 nM for 10 min, followed by stimulation with 10 nM insulin for 30 min. Pretreatment with calyculin A enhanced the phosphorylation of IRS-1 in WT MEF cells in a dose-dependent manner, whereas little effect was observed in PRIP-KO MEF cells (Fig. 6B), indicating that PP1 and/or PP2A are involved in the dephosphorylation of IRS-1 in MEF cells from WT mice. In contrast, PP1 and/or PP2A were non-accessible to IRS-1 as a substrate in the absence of PRIP. To exclude the possibility that increased IRS-1 serine phosphorylation in PRIP-KO cells is merely due to the upregulation of IRS-1 phosphorylation instead of suppressed dephosphorylation, we also examined the phosphorylation of p70S6K (encoded by *Rps6kb1*), which is activated upon Akt activation. Our results showed that phosphorylation of p70S6K upon insulin stimulation was also inhibited, suggesting that dephosphorylation by PP1 and/or PP2A is suppressed in PRIP-KO cells (Fig. S2B). Next, we examined the interaction between IRS-1 and PP1 or PP2A in the presence or absence of PRIP using proximity ligation assay (PLA) technology. Adipocytes differentiated from MEF cells of WT mice were probed with a combination of rabbit antibody against IRS-1 and mouse antibody against control IgG, PP1 or PP2Ac (catalytic subunit of PP2A) as a primary antibody, followed by further probing with PLA probes for mouse and rabbit primary antibodies, ligation and amplification reactions. As shown in Fig. 6C, red fluorescent spots indicating the colocalisation of two proteins were only detected in cells that were probed using antibodies against IRS-1 and PP2Ac. The MEF-derived adipocytes from WT and KO mice were also assayed as described above. Our findings demonstrated that red fluorescent spots indicating the interaction of IRS-1 and PP2A were more evident in WT adipocytes, whereas they were dramatically decreased in PRIP-KO adipocytes (Fig. 6D). Based on these results, we concluded that PRIP acts as a scaffold protein that recruits PP2A to IRS-1 to induce its dephosphorylation.

DISCUSSION

In the present study, we showed that the ablation of PRIP led to impaired insulin signalling and insulin-mediated cellular functions in adipocytes, including reduction of insulin-stimulated phosphorylation of IR, IRS-1 and Akt, as well as of insulin-induced glucose uptake. Although many mechanisms negatively regulate the insulin signalling pathway, including impaired IR–IRS-1 interactions, degradation of IRS-1 and increased protein expression of phosphatidylinositol (3,4,5)-trisphosphate [PtdIns(3,4,5)P3] phosphatases, such as PTEN (Paz et al., 1997; Kim et al., 2005; Nawaratne et al., 2006; Shah et al., 2004; Nakashima et al., 2000), we focused on whether the cell surface expression level of IR was involved in the downregulation of insulin-induced cellular events by PRIP, because the phosphorylation of IR was impaired in PRIP-deficient adipocytes. Indeed, in the absence of PRIP, serine phosphorylation of IRS-1 was increased because of the aberrant dephosphorylation of IRS-1, which in turn resulted in enhanced IR endocytosis. Our results suggest that PRIP blocks the clathrin-dependent constitutive internalisation of IR by binding to IR and recruiting PP2A to IRS-1 to induce its dephosphorylation, which maintains the amount of IR on the cell surface at a moderate level for the sustained activation of insulin signalling (Fig. 7).

Choi et al. (2019) have reported that the phosphorylation of IRS-1 at serine 612 by ERK1/2 induces Src homology phosphatase 2 (SHP2, also known as PTPN11) to dephosphorylate tyrosine 608, which promotes the association of IRS-1 with AP2, resulting in the enhanced internalisation of IR. Indeed, the experimental phosphorylation of serine 612 in addition to other sites by treating cells with PMA reduced cell surface IR without affecting the amount of IRS-1 in our study. Therefore, elevated serine 612 phosphorylation in adipocytes from PRIP-KO mice might be involved in the enhanced internalisation of IR. However, phosphorylation of serine 632 and serine 1097 on IRS-1 is mediated by mTORC1 and p70S6K, respectively, the chronic activation of which induces the degradation of IRS-1 and subsequent insulin resistance (Harrington et al., 2004; Shah et al., 2004). Furthermore, Yoneyama et al. (2018b) have reported that IRS-1 inhibits the clathrin- and AP2-dependent internalisation of insulin-like growth factor-1 receptor (IGF-1R), which enhances the surface retention of activated IGF-1R in rat L6 cells. Although the reduction of IRS-1 levels was not observed in our study, these reports suggest that the prolonged phosphorylation of IRS-1 at serine 632 and serine 1097 might induce the degradation of IRS-1 followed by further enhancement of IR internalisation. Experiments using mutant IRS-1 with site-directed mutagenesis of these serine residues might determine whether the phosphorylation of these residues is involved in the control of IR internalisation by PRIP.

Journal of Cell Science (2022) 135, jcs258584. doi:10.1242/jcs.258584

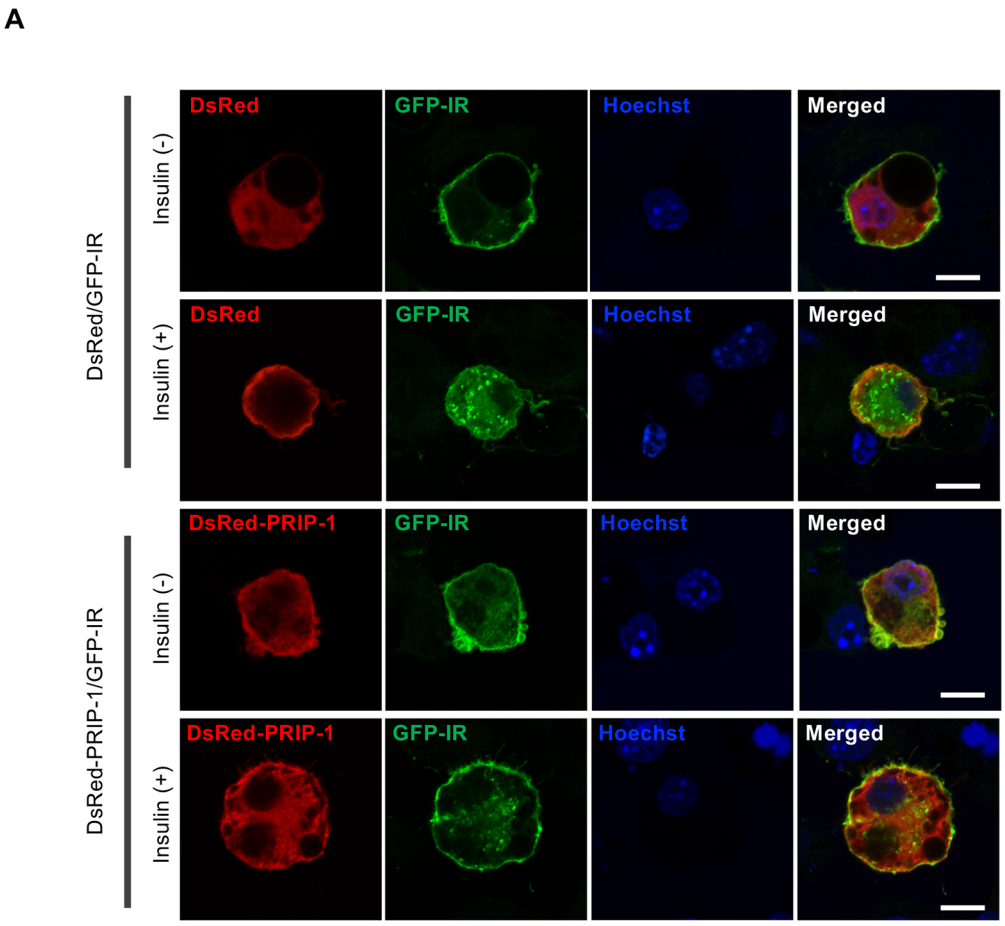

Fig. 4. Internalisation of IR induced by insulin is inhibited by the overexpression of PRIP-1. (A) 3T3-L1 adipocytes were transfected with constructs for the expression of GFP–IR and either DsRed or DsRed–PRIP-1. After serum-starvation for 6 h, the cells were stimulated with 20 nM insulin for 15 min, followed by fixation with 4% PFA, and subjected to immunocytochemistry using anti-GFP and anti-RFP antibodies. Nuclei were stained using Hoechst 33258. Representative images of four experiments are shown. Scale bars: 10 µm. (B) HepG2 cells stably expressing GFP or GFP–PRIP-1 were lysed and subjected to immunoprecipitation (IP) using anti-GFP antibodies. Immunocomplexes were separated by SDS–PAGE and analysed by western blotting using the indicated antibodies. Input lanes represent 0.3% of the total lysate. The panels show typical immunoblots, representative of three experiments.

Currently, the mechanism of how the phospho-status of these serine residues on IRS-1 is maintained has not been clarified in detail. However, our data suggests that PRIP recruits PP2A to IRS-1 by interacting with IR, either directly or indirectly, to dephosphorylate the phosphorylation of serine at the 612, 632 and 1097 residues so that the phosphorylation level of IRS-1 is maintained at an appropriate level.

In addition to the regulation of IR endocytosis by controlling the phosphorylation of IRS-1, PRIP might affect phosphorylation of Akt through other mechanisms. We have previously reported that the phosphorylation of Akt induced by platelet-derived growth factor (PDGF) or lipopolysaccharide (LPS) is enhanced in fibroblasts or microglia from PRIP-KO mice, respectively (Asano et al., 2017; Yamawaki et al., 2019). In those cases, PRIP interacts

Journal of Cell Science (2022) 135, jcs258584. doi:10.1242/jcs.258584

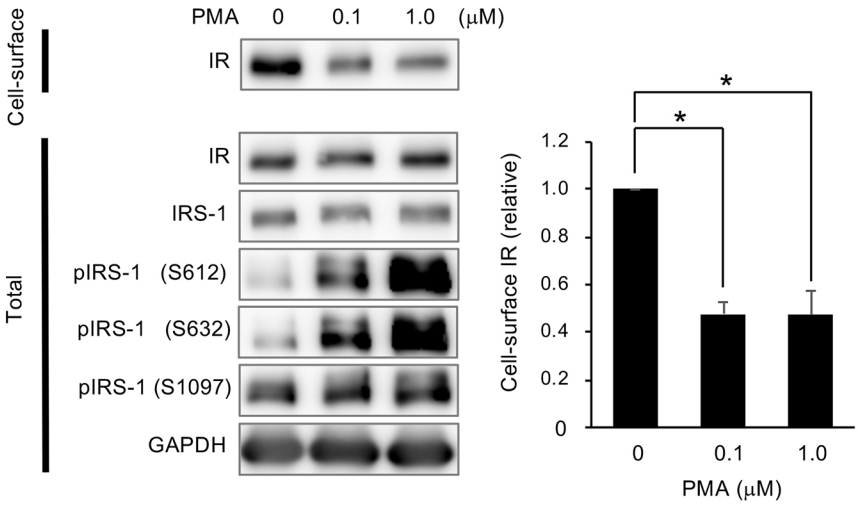

Fig. 5. Serine phosphorylation of IRS-1 promotes the internalisation of IR. 3T3L1 cells were cultured in 6-well plates and differentiated to adipocytes. A cell surface biotinylation assay was performed after cells were treated with the indicated concentrations of PMA. Cell surface biotinylated proteins associated with NeutraAvidin beads and total cell lysates were subjected to SDS–PAGE and western blotting with antibodies to detect the indicated proteins and phosphoproteins. GAPDH is shown as a loading control. Representative blots and quantitative data are shown. Data are the mean±s.e.m. from four independent experiments. *P<0.05, versus the corresponding no stimulation value (Mann–Whitney test).

with PtdIns(4,5)P_2 through its pleckstrin homology (PH) domain and interferes with the access of phosphoinositide 3-kinase (PI3K) to its substrate PtdIns(4,5)P_2, which sequesters the metabolic conversion of PtdIns(4,5)P_2 to PtdIns(3,4,5)P_3, leading to inhibition of Akt activation (Asano et al., 2017). However, this process is downstream of IRS-1 in the insulin signalling pathway, and the mechanism that regulates the internalisation of IR and affects insulin signalling by PRIP is upstream of PI3K. Furthermore, the conclusion of this study is based on the regulation of dephosphorylation of serine phosphorylation of IRS-1 by PRIP, which in turn controls receptor internalisation. To the best of our knowledge, there are no reports indicating that the serine or threonine phosphorylation of IRS-1 induced by PDGF or LPS could promote internalisation of their receptors. Therefore, the results obtained in this study regarding insulin signalling are not contrary to the results obtained using other stimuli in our previous reports.

Because insulin-induced glucose uptake was downregulated in cultured PRIP-KO adipocytes, we speculated that systemic glucose metabolism was impaired in PRIP-KO mice. However, our results have revealed that PRIP-KO mice do not show impaired glucose or insulin tolerance as compared with WT mice (Fig. S3). This might be partially attributed to the enhanced insulin secretion in response to glucose administration in PRIP-KO mice, because PRIP is involved in the regulation of insulin secretion in pancreatic islets (Fig. S4) (Asano et al., 2014). PRIP is a scaffold protein that binds to several proteins. In addition to its function as a positive regulator to facilitate insulin signalling in WAT, PRIP also promotes whole-body energy metabolism by negatively regulating UCP-1-mediated thermogenesis in brown adipose tissue, which helps control systemic insulin sensitivity (Oue et al., 2016). This might explain why the PRIP-KO mice did not show whole-body insulin resistance.

The impaired action of insulin, such as the insensitivity of insulin signalling in adipose tissues, reduces the synthesis of triacylglycerol and increases lipolysis. Indeed, we have previously reported that PRIP-KO mice have a lean phenotype (Okumura et al., 2014; Oue et al., 2016). We have shown that lipolysis is enhanced in the adipose tissues of PRIP-KO mice, resulting in elevated plasma free non-esterified fatty acids (NEFA) but without the manifestation of fatty liver. This phenotype is consistent with the finding in this study that insulin signalling is inhibited in PRIP-KO mice, which promotes lipolysis and reduces the synthesis of triacylglycerol. The loss of adipose tissue mass is tightly associated with the dysregulation of metabolism, including insulin resistance (Bindlish et al., 2015; Romere at al., 2016). A deficiency of Akt1 and Akt2 or of IRs in adipocytes causes severe lipodystrophy with fatty liver and systemic insulin resistance (Shearin et al., 2016; Softic et al., 2016). Although the phenotype of PRIP-KO mice is not as obvious as that of Akt1 and Akt2-KO mice, both show a reduction in the size of WAT. The ablation of PRIP causes adipocyte cell-autonomous desensitisation of insulin signalling, which is different from obesity-induced systemic insulin resistance.

In conclusion, we showed that PRIP inhibited the internalisation of IR on the plasma membrane, possibly by binding to IR and promoting the dephosphorylation of IRS-1 serine phosphorylation in adipocytes. We report a novel role for PRIP that positively maintains insulin signalling in adipocytes. Because adipose tissues are critical for the regulation of metabolism, whose perturbation is closely associated with obesity and related disorders, this finding will provide new insights into the pathogenesis of obesity and its associated diseases, as well as drug discovery.

MATERIALS AND METHODS

Animals

PRIP-1 and PRIP-2 double KO (PRIP-KO) mice on a C57BL/6J (The Jackson Laboratory, Bar Harbor, ME) background were generated as described previously (Kanematsu et al., 2006). Mice were maintained under specific pathogen-free (SPF) conditions with a 12-h light:12-h dark cycle. The handling of mice was approved by the Institutional Animal Care and Use Committee of Kyushu University, and all the procedures were performed according to the Guidelines for Proper Conduct of Animal Experiments of the Science Council of Japan.

Reagents and antibodies

Insulin, primaquine, phorbol 12-myristate 13-acetate (PMA) and calyculin A were from Merck Millipore. Rapamycin was from LC Laboratories. Antibodies used were as follows: anti-IR (#3025, 1:1000), anti-phosphoIRS-1 (Ser1101) (#2385, 1:1000), anti-phosphoIRS-1 (Ser612) (#3203, 1:1000), anti-phosphoIRS-1 (Ser632) (#2388, 1:1000), anti-Akt1 (#9272, 1:1000), anti-phosphoAkt1 (Thr308) (#13038, 1:1000), anti-GAPDH (#2118, 1:1000), anti-Rab5 (#3547, 1:1000), anti-GLUT4 (#2213, x1000), anti-adiponectin (#2789, 1:1000), anti-phosphoS6K (T389) (#9234, 1:1000) and PPARγ (#2443, 1:1000) antibodies were obtained from Cell Signaling Technology. Anti-PP1 (SC-74882, 1:100), anti-IRS-1 (SC-559, 1:50) and anti-GFP (SC-8334, 1:50) (for immunofluorescence) antibodies were purchased from Santa Cruz Biotechnology. Anti-PP2A catalytic α (#05-421, 1:200), anti-IRS-1 (#06-248, 1:1000 for immunoblotting), anti-β-actin (A5441, 1:3000) antibody were from Merck Millipore. Anti-phosphoIR (Y1361) (ab60946, 1:1000) antibody was from Abcam. Anti-phosphoIRS-1

Journal of Cell Science (2022) 135, jcs258584. doi:10.1242/jcs.258584

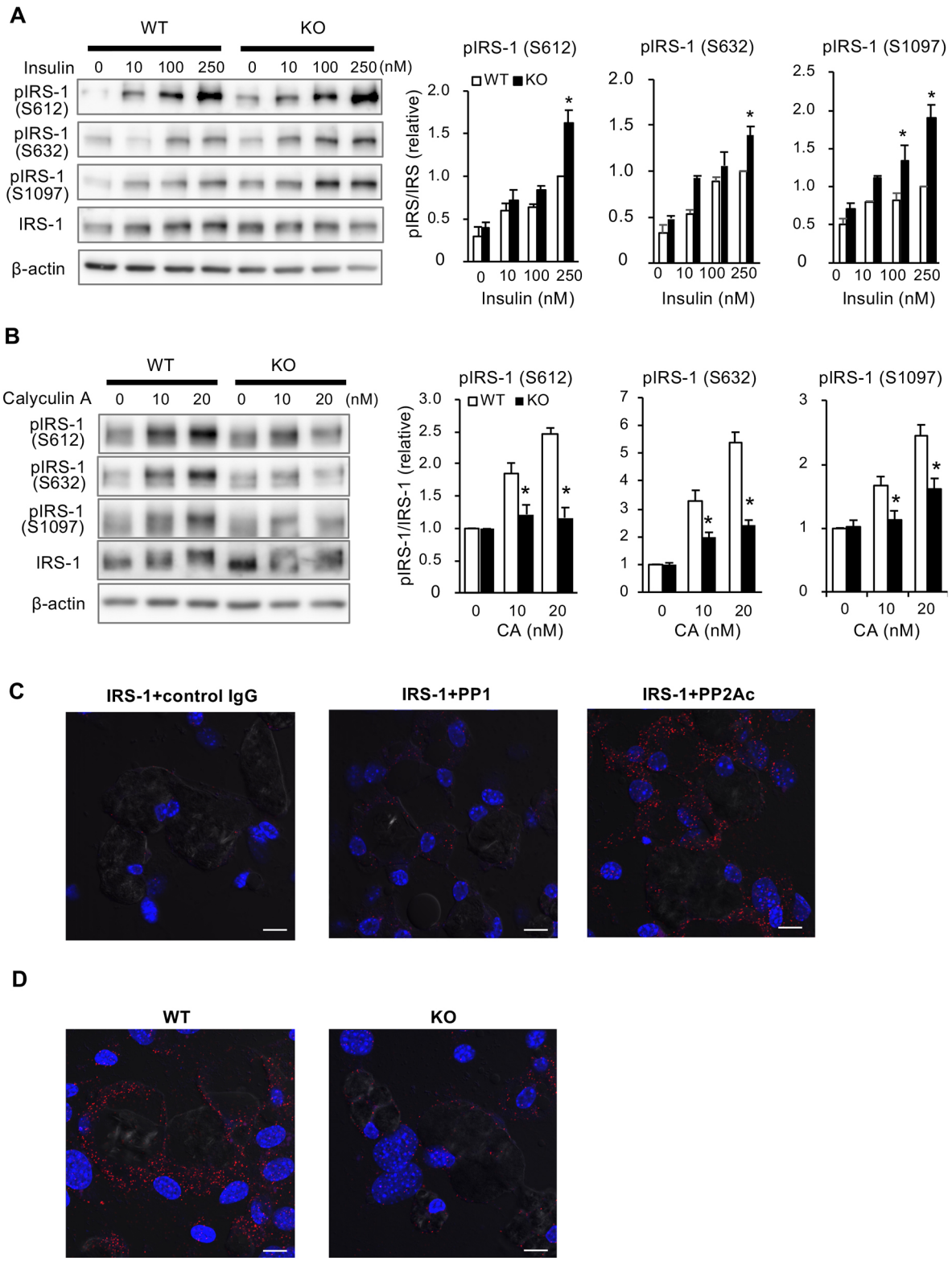

Fig. 6. See next page for legend.

(Y608) (#44816, 1:1000) antibody was from Thermo Fisher Scientific. Anti-GFP antibody (for immunoprecipitation, 1:300) was from Fujifilm Wako. Anti-HA (M180-3, 1:500) and anti-RFP (M165-3, 1:200) were from MBL.

Constructs and siRNA

Plasmids expressing full-length PRIP were constructed in pSG5, phGFP 105/Sse and pDsRed N1 vectors in mammalian cells as described previously (Takeuchi et al., 2000; Kanematsu et al., 2006). The plasmid construct insulin receptor/pEGFP-N2 was purchased from Addgene (Addgene 22286 Ramos et al., 2007). Human GLUT4 cDNA containing an HA epitope tag in the first exofacial loop was kindly gifted by Prof. Sun Sik Bae (Pusan National University, Busan, Korea). HA–GLUT4 was constructed in the pEGFP-N1 vector, as described previously (Nagano et al., 2015). siRNA against mouse Rab5a (271457), Rab5b (19344), Rab5c (19345), PRIP-1

Fig. 6. Serine phosphorylation of IRS-1 is regulated by PRIP by modulating the dephosphorylation of IRS-1. (A) MEF cells isolated from WT and PRIP-KO mice were seeded in a 12-well plate at 8×10^4 cells/well and cultured for 24 h. After serum starvation for 12–14 h, cells were stimulated with insulin at the indicated concentrations for 30 min. The extracted cell lysates were analysed by SDS–PAGE and western blotting using antibodies to detect the indicated proteins and phosphoproteins. (B) MEF cells isolated from WT and PRIP-KO mice were seeded in a 12-well plate at 8×10^4 cells/well and cultured for 24 h. Cells were treated with calyculin A (CA) at the indicated concentrations for 10 min, followed by stimulation with 10 nM insulin for 30 min. The extracted cell lysates were analysed by SDS–PAGE and western blotting using antibodies to detect the indicated proteins and phosphoproteins. The immunoblotting of IRS-1 phosphorylation at serine 632 was performed after stripping the serine 612 membrane and re-probing with anti-pIRS-1 (Ser632) antibody. In A and B, representative blots and quantitative data are shown. β-actin is shown as a loading control. Data are the mean±s.e.m. from four independent experiments. *P<0.05, versus the corresponding WT value (Mann–Whitney test). (C) WT MEF cells cultured on coverslips were differentiated to adipocytes and subjected to PLA assay using a combination of antibodies against IRS-1 and control IgG, PP1 or PP2Ac. PLA signals are shown in red, and nuclei counterstained with DAPI are shown in blue. (D) MEF cells from WT and PRIP-KO mice cultured on coverslips were differentiated to adipocytes and subjected to PLA assay using a combination of antibodies against IRS-1 and PP2Ac. Typical merged images showing PLA signals (red), DAPI (blue) and differential interference contrast signals are shown. Images in C and D are representative of four experiments. Scale bars: 10 µm.

(227120) and PRIP-2 (224860) were from the Dharmacon ON-TARGETplus siRNA SMART pool (GE Healthcare).

Cell culture and transfection

Mouse embryonic fibroblasts (MEFs) were established from WT and PRIP-KO mice E13.5 embryos following standard protocol (Choi et al., 2016). 3T3-L1 cells and HepG2 cells were initially purchased from JCRB cell bank (Tokyo, Japan) and maintained in mycoplasma-free culture. 3T3-L1 cells and HepG2 cells were cultured in Dulbecco's Modified Eagle's Medium (DMEM, 4500 mg/l glucose for 3T3L1 and 1000 mg/l glucose for HepG2, respectively; Merck Millipore) containing 10% calf serum (CS; GE Healthcare) or 10% fetal bovine serum (FBS; Thermo Fisher Scientific) (for 3T3L1 and HepG2 cells, respectively), 100 U/ml penicillin and 100 µg/ml streptomycin in a humidified atmosphere containing 5% CO_2 at 37°C. For the induction of adipogenic differentiation, MEFs or 3T3-L1 cells were plated in 6-well plates and propagated to confluency. Two days later, the medium was replaced with standard differentiation induction medium (DMEM supplemented with 10% FBS) containing 0.25 µM dexamethasone (Merck Millipore), 0.5 µM IBMX (Merck Millipore), 10 µM troglitazone (Merck Millipore) and 166 nM insulin. Three to five days later, the medium was changed to that containing only insulin for another two to four days. For MEFs, this cycle was repeated until cytoplasmic lipid accumulation was observed in more than 30% of the cells, as observed by bright-field microscopy. For Oil Red O staining, cells were stained with 60% filtered Oil Red O in isopropanol for 30 min at room temperature after fixing in 4% PFA.

The indicated plasmid DNAs and siRNAs were transfected into cells using Lipofectamine 3000 and Lipofectamine RNAiMax according to the manufacturer's instructions (Invitrogen, Thermo Fisher Scientific, MA, USA), respectively. Cells were transfected with 100 µM siRNA using RNAiMAX at the time of changing the medium to that containing only insulin, and relevant assays were performed two days later.

HepG2 clonal cells stably expressing GFP and GFP–PRIP-1 were generated as follows: HepG2 cells were first transfected with phGFP105 or PRIP-1 (wild type)/phGFP105 (Takeuchi et al., 2000) using Lipofectamine 3000. Transfected cells were maintained in growth medium containing 2000 µg/ml G418 (Thermo Fisher Scientific) for approximately a month. The growing colonies were visually selected for GFP fluorescence analysis.

Quantitative RT-PCR analysis

Total RNA was extracted from 3T3L1 adipocytes using an ReliaPrep RNA Miniprep System (Promega) and was subjected to reverse transcription with High-Capacity cDNA RT Kit (Thermo Fisher Scientific). The resulting cDNA was subjected to real-time PCR analysis with KOD SYR qPCR Mix (TOYOBO) in a Takara PCR Thermal Cycler Dice Gradient instrument (Takara Bio). Specific primers for PRIP-1 and PRIP-2 were follows: PRIP-1 forward, 5′-TCCTGGAGGCTGCACGAG-3′; PRIP-1 reverse, 5′-TGAAGCTAATGCAGTCGTGG-3′; PRIP-2 forward, 5′-CCCAGGGA-CAGCAAACCG-3′; PRIP-2 reverse, 5′-TGAGTTGATACAGT-CACTTGC-3′.

Immunoprecipitation and immunoblotting

Cultured cells were lysed in ice-cold lysis buffer (50 mM Tris-HCl at pH 7.5, 150 mM NaCl, 5 mM EDTA, 1% Triton X-100, 1 mM DTT) supplemented with a phosphatase inhibitor cocktail (Nacalai Tesque) and a protease inhibitor cocktail (Merck Millipore). The lysates were subjected to immunoprecipitation with specific antibodies and Protein G–Sepharose beads, and the bead-bound proteins were fractionated by SDS–PAGE and transferred to a PVDF membrane (Merck Millipore). After the blocking of nonspecific sites with 5% dried skim milk, the membrane was incubated with primary antibodies and then with HRP-conjugated sheep or donkey secondary antibodies (GE Healthcare). Immune complexes were detected with enhanced chemiluminescence reagents (GE Healthcare), and chemiluminescence signals were detected with an LAS-4000 imaging system (Fujifilm, Tokyo, Japan). Digital images were analysed with ImageQuant TL software (Fujifilm) to measure band intensity.

Immunofluorescence and PLA

Immunocytochemical analysis was performed as described previously (Gao et al., 2012). Cells were plated on poly-L-lysine-coated glass coverslips in a 12-well plate and cultured for 24 h. They were then fixed for 30 min at 4°C with 4% PFA in phosphate-buffered saline (PBS), permeabilised for 8 min at 25°C with 0.2% Triton X-100 and exposed to 1% bovine serum albumin to block nonspecific sites. Immunostaining was performed for 2 h at room temperature with primary antibodies in PBS containing 0.1% bovine serum albumin. Immune complexes were detected by the incubation of cells with Alexa Fluor 488-conjugated donkey antibodies to rabbit IgG and Alexa Fluor 594-conjugated goat antibodies to mouse IgG (each diluted 1:400) for 40 min at room temperature. Cells on the coverslips were mounted on slides using Permafluor (Beckman Coulter, Fullerton, CA) and observed with a laser confocal microscope (LSM 510; Carl Zeiss, Jena, Germany).

In situ PLA was performed using a Duolink *in situ* kit following the manufacturer's protocol; however, the cells were prepared and permeabilised using the method used for immunofluorescence studies. Briefly, two molecules present in permeabilised cells were recognised by their respective primary antibodies raised in mice or rabbits, respectively, and secondary antibodies to mouse or rabbit Ig conjugated with a unique short DNA strand was then added, followed by the ligation of these secondary antibodies and amplification of the ligates. When two molecules were close, within 40 nm, successful ligation and amplification were performed for further analysis. Confocal images were obtained using LSM510 META (Carl Zeiss).

Biotinylation assay

Cells were placed on ice and washed with PBS containing Ca^{2+} and Mg^{2+} at 1 mM and 0.5 mM, respectively. Then, cells were incubated for 30 min with PBS containing 1 mg/ml EZ-link sulfo-NHS-LC-biotin (Thermo Fisher Scientific) prepared just before use. Cells were washed three times with ice-cold PBS containing lysine (100 mM) and immediately lysed with ice-cold lysis buffer containing phosphatase and protease inhibitors as described above. Cell lysates were mixed with Pierce Streptavidin UltraLink Resin (Thermo Fisher Scientific) for 1.5 h at 4°C to form an Avidin–Biotin complex (ABC). The ABC resin was washed with lysis buffer 3–4 times, and the precipitated proteins were analysed by western blotting.

Glucose uptake assay

Epididymal WAT was dissected from mice, cut into pieces of 1–2 mm^2, and incubated in M199 medium (Merck Millipore) without serum overnight at 37°C in 5% CO_2. The cut WAT was then washed with Krebs Ringer

Journal of Cell Science (2022) 135, jcs258584. doi:10.1242/jcs.258584

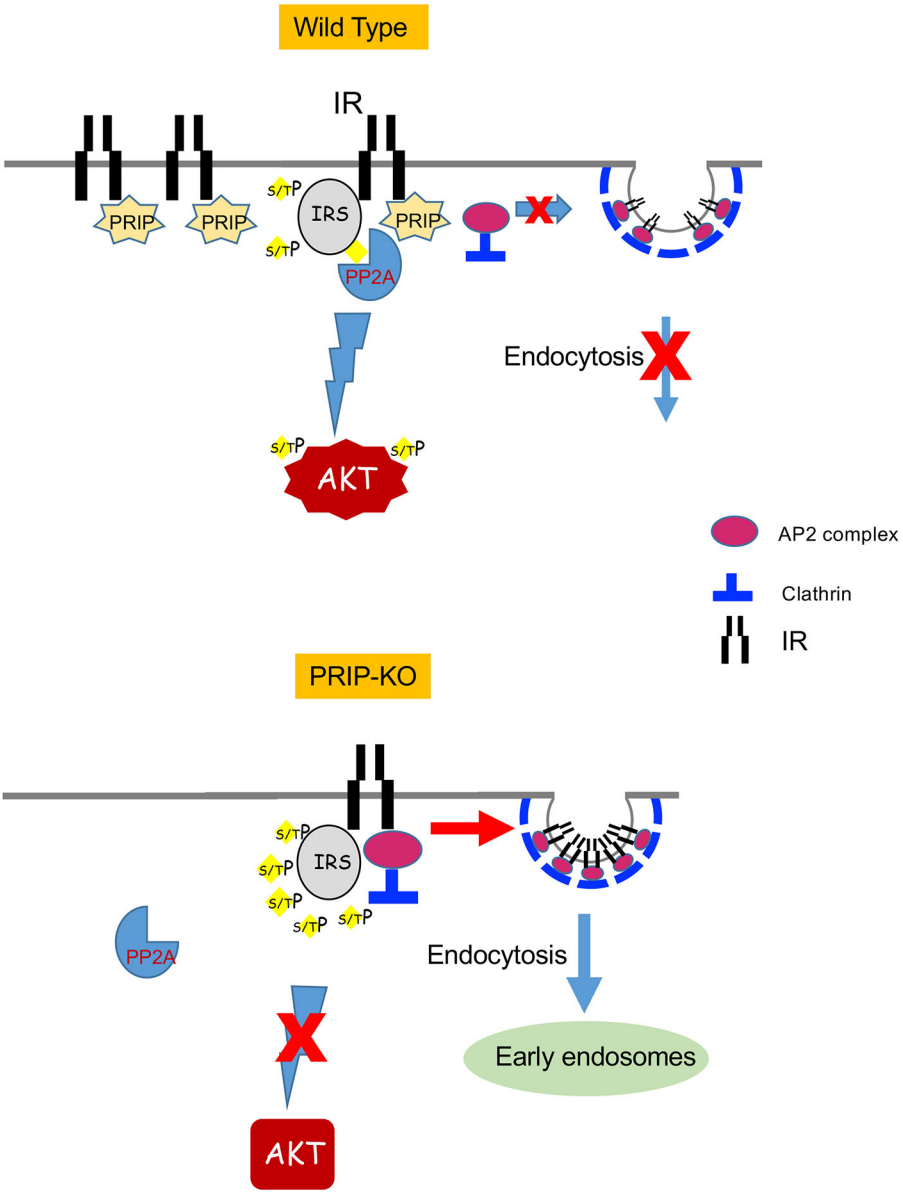

Fig. 7. Schematic representation of the PRIP-mediated control of insulin signalling in adipocytes. PRIP, IR and IRS-1 (IRS) form a complex, and PRIP blocks the AP2 and clathrin-mediated constitutive endocytosis of IR. PRIP recruits PP2A to IRS-1 to dephosphorylate serine phosphorylated ($_{S/T}$P) IRS-1. Thus, PRIP acts as a positive regulator of the insulin signalling pathway by maintaining an appropriate amount of IR on the plasma membrane. In the absence of PRIP, IR is subjected to internalisation by AP2 and clathrin. The serine phosphorylation level of IRS-1 is enhanced because PP2A cannot be recruited to IRS-1, which promotes the internalisation of IR even without insulin stimulation, resulting in diminished numbers of IRs on the plasma membrane and reduced insulin signalling.

Phosphate HEPES (KRPH) buffer (1.2 mM KH_2PO_4, 1.2 mM $MgSO_4$, 1.3 mM $CaCl_2$, 118 mM NaCl, 5 mM KCl, 30 mM HEPES, pH 7.5) at 37°C and treated with 20 nM insulin for 18 min, followed by incubation with 1 mM 2-deoxyglucose (2-DG; Merck Millipore) for 20 min and washing three times with PBS containing 10 µM cytochalasin B (Fujifilm Wako). Tissue samples were lysed by sonication lysis buffer supplied in the Glucose Cellular Uptake Measurement Kit (Cosmo Bio). The intracellular 2-DG-6-phosphate levels were measured according to the manufacturer's instructions. Glucose uptake into the MEF-derived adipocytes was also measured using the same kit.

GLUT4 translocation assay

3T3-L1 adipocytes were transiently co-transfected with the plasmid construct expressing HA–GLUT4–EGFP and either siRNAs against PRIP-1 and -2 or control scramble siRNA. Two days later, cells were stimulated with 20 nM insulin for 15 min after 6 h of serum starvation, followed by fixation without any permeabilisation. Exofacial HA exposure on the outside of cells was visualised by immunostaining using an anti-HA antibody (MBL) followed by incubation of cells with Alexa Fluor 594-conjugated goat secondary antibody. Confocal images were obtained using an LSM510 META microscope (Carl Zeiss).

Metabolic measurement

A glucose tolerance test (GTT) and assessment of glucose-stimulated insulin secretion (GSIS) were performed after subjecting the mice (male mice at 12–13 weeks of age) to fasting for 18 h. Glucose (1 g/kg) was injected intraperitoneally, and blood glucose concentration was measured at various time points thereafter using free style lite blood glucose test strips (Abbott Laboratories, IL, USA). For GSIS, blood samples were collected at time 0 for fasting insulin measurements and at 15 min post glucose injection. Serum isolated from the blood samples was assayed for insulin using an ELISA kit obtained from Mercodia AB, Uppsala, Sweden. An insulin tolerance test (ITT) was performed after subjecting the mice to 4 h of fasting. Insulin (0.5 U/kg) (Humulin R; Eli Lily) was injected intraperitoneally, and blood glucose concentration was measured at various time points thereafter. HOMA-IR was calculated using an online calculator on the Diabetes Trials Unit of the University of Oxford website (https://www.dtu.ox.ac.uk/homacalculator/).

Statistical analysis

Quantitative data are presented as the means±s.e.m., and comparisons were performed between or among groups using the Mann–Whitney test, two-way

ANOVA with Tukey's HSD post hoc test for multiple comparisons, or two-tailed unpaired Student's *t*-test, analysed using JMP Pro 15.1.0, SAS Institute Inc. (Cary, NC, USA).

Acknowledgements
We thank J. Ludovic Croxford, PhD, from Edanz Group (https://en-author-services.edanzgroup.com/ac) for editing a draft of this manuscript. We thank the Research Support Center, Graduate School of Medical Sciences, Kyushu University, for technical support. We thank Professor Sun Sik Bae (Pusan National University, Korea) for providing us with human GLUT4 cDNA containing an HA epitope tag in the first exofacial loop.

Competing interests
The authors declare no competing or financial interests.

Author contributions
Conceptualization: J.G., A.M., H.T., M.H.; Methodology: J.G., A.M., H.T.; Investigation: J.G., A.M., A.L., F.H., H.N.; Data curation: J.G., A.M.; Writing - original draft: J.G., M.H.; Writing - review & editing: J.G., A.M., H.T., T.K., E.J., M.H.; Visualization: J.G.; Supervision: H.T., T.K., M.H.; Project administration: J.G., H.T., M.H.; Funding acquisition: J.G., M.H.

Funding
This work was supported by the Japan Society for the Promotion of Science (KAKENHI grants 16K11479 and 19K10054 to J.G., 17K11649 to H.T., 20H03854 to M.H.).

References

Asano, S., Nemoto, T., Kitayama, T., Harada, K., Zhang, J., Harada, K., Tanida, I., Hirata, M. and Kanematsu, T. (2014). Phospholipase C-related catalytically inactive protein (PRIP) controls KIF5B-mediated insulin secretion. *Biol. Open* **3**, 463-474. doi:10.1242/bio.20147591

Asano, S., Taniguchi, Y., Yamawaki, Y., Gao, J., Harada, K., Takeuchi, H., Hirata, M. and Kanematsu, T. (2017). Suppression of cell migration by phospholipase C-related catalytically inactive protein-dependent modulation of PI3K signalling. *Sci. Rep.* **7**, 5408. doi:10.1038/s41598-017-05908-7

Bindlish, S., Presswala, L. S. and Schwartz, F. (2015). Lipodystrophy: syndrome of severe insulin resistance. *Postgrad. Med.* **127**, 511-516. doi:10.1080/00325481.2015.1015927

Boucher, J., Kleinridders, A. and Kahn, C. R. (2014). Insulin receptor signaling in normal and insulin-resistant state. *Cold Spring Harb. Perspect. Biol.* **6**, a009191. doi:10.1101/cshperspect.a009191

Choi, E., Zhang, X., Xing, C. and Yu, H. (2016). Mitotic checkpoint regulators control insulin signaling and metabolic homeostasis. *Cell* **166**, 567-581. doi:10.1016/j.cell.2016.05.074

Choi, E., Kikuchi, S., Gao, H., Brodzik, K., Nassour, I., Yopp, A., Singal, A. G., Zhu, H. and Yu, H. (2019). Mitotic regulators and the SHP2-MAPK pathway promote IR endocytosis and feedback regulation of insulin signaling. *Nat. Commun.* **10**, 1473. doi:10.1038/s41467-019-09318-3

Copps, K. D. and White, M. F. (2012). Regulation of insulin sensitivity by serine/threonine phosphorylation of insulin receptor substrate proteins IRS1 and IRS2. *Diabetologia* **55**, 2565-2582. doi:10.1007/s00125-012-2644-8

Fujii, M., Kanematsu, T., Ishibashi, H., Fukami, K., Takenawa, T., Nakayama, K. I., Moss, S. J., Nabekura, J. and Hirata, M. (2010). Phospholipase C-related but catalytically inactive protein is required for insulin-induced cell surface expression of γ-aminobutyric acid type A receptors. *J. Biol. Chem.* **285**, 4837-4846. doi:10.1074/jbc.M109.070045

Gao, J., Takeuchi, H., Zhang, Z., Fujii, M., Kanematsu, T. and Hirata, M. (2009). Binding of phospholipase C-related but catalytically inactive protein to phosphatidylinositol 4,5-bisphosphate via the PH domain. *Cell. Signal.* **21**, 1180-1186. doi:10.1016/j.cellsig.2009.03.008

Gao, J., Takeuchi, H., Zhang, Z., Fukuda, M. and Hirata, M. (2012). Phospholipase C-related but catalytically inactive protein (PRIP) modulates synaptosomal-associated protein 25 (SNAP-25) phosphorylation and exocytosis. *J. Biol. Chem.* **287**, 10565-10578. doi:10.1074/jbc.M111.294645

Goh, L. K. and Sorkin, A. (2013). Endocytosis of receptor tyrosine kinases. *Cold Spring Harb. Perspect. Biol.* **5**, a017459. doi:10.1101/cshperspect.a017459

Harada, K., Takeuchi, H., Oike, M., Matsuda, M., Kanematsu, T., Yagisawa, H., Nakayama, K.-I., Maeda, K., Erneux, C. and Hirata, M. (2005). Role of PRIP-1, a novel $Ins(1,4,5)P_3$ binding protein, in $Ins(1,4,5)P_3$-mediated Ca^{2+} signaling. *J. Cell. Physiol.* **202**, 422-433. doi:10.1002/jcp.20136

Harrington, L. S., Findlay, G. M., Gray, A., Tolkacheva, T., Wigfield, S., Rebholz, H., Barnett, J., Leslie, N. R., Cheng, S., Shepherd, P. R. et al. (2004). The TSC1-2 tumor suppressor controls insulin-PI3K signaling via regulation of IRS proteins. *J. Cell Biol.* **166**, 213-223. doi:10.1083/jcb.200403069

Kanematsu, T., Takeya, H., Watanabe, Y., Ozaki, S., Yoshida, M., Koga, T., Iwanaga, S. and Hirata, M. (1992). Putative inositol 1,4,5-trisphosphate binding proteins in rat brain cytosol. *J. Biol. Chem.* **267**, 6518-6525. doi:10.1016/S0021-9258(19)50458-6

Kanematsu, T., Jang, I.-S., Yamaguchi, T., Nagahama, H., Yoshimura, K., Hidaka, K., Matsuda, M., Takeuchi, H., Misumi, Y., Nakayama, K. et al. (2002). Role of the PLC-related, catalytically inactive protein p130 in GABAA receptor function. *EMBO J.* **21**, 1004-1011. doi:10.1093/emboj/21.5.1004

Kanematsu, T., Yasunaga, A., Mizoguchi, Y., Kuratani, A., Kittler, J. T., Jovanovic, J. N., Takenaka, K., Nakayama, K. I., Fukami, K., Takenawa, T. et al. (2006). Modulation of $GABA_A$ receptor phosphorylation and membrane trafficking by phospholipase C-related inactive protein/protein phosphatase 1 and 2A signaling complex underlying brain-derived neurotrophic factor-dependent regulation of GABAergic inhibition. *J. Biol. Chem.* **281**, 22180-22189. doi:10.1074/jbc.M603118200

Kim, J. A., Yeh, D. C., Ver, M., Li, Y., Carranza, A., Conrads, T. P., Veenstra, T. D., Harrington, M. A. and Quon, M. J. (2005). Phosphorylation of Ser24 in the pleckstrin homology domain of insulin receptor substrate-1 by Mouse Pelle-like kinase/interleukin-1 receptor-associated kinase: cross-talk between inflammatory signaling and insulin signaling that may contribute to insulin resistance. *J. Biol. Chem.* **280**, 23173-23183. doi:10.1074/jbc.M501439200

Knutson, V. P. (1991). Cellular trafficking and processing of the insulin receptor. *FASEB J.* **5**, 2130-2138. doi:10.1096/fasebj.5.8.2022311

Lemmon, M. A. and Schlessinger, J. (2010). Cell signaling by receptor-tyrosine kinases. *Cell* **141**, 1117-1134. doi:10.1016/j.cell.2010.06.011

Nagano, K., Takeuchi, H., Gao, J., Mori, Y., Otani, T., Wang, D. G. and Hirata, M. (2015). Tomosyn is a novel Akt substrate mediating insulin-dependent GLUT4 exocytosis. *Int. J. Biochem. Cell Biol.* **62**, 62-71. doi:10.1016/j.biocel.2015.02.013

Nakashima, N., Sharma, P. M., Imamura, T., Bookstein, R. and Olefsky, J. M. (2000). The tumor suppressor PTEN negatively regulates insulin signaling in 3T3-L1 adipocytes. *J. Biol. Chem.* **275**, 12889-12895. doi:10.1074/jbc.275.17.12889

Nawaratne, R., Gray, A., Jørgensen, C. H., Downes, C. P., Siddle, K. and Sethi, J. K. (2006). Regulation of insulin receptor substrate 1 pleckstrin homology domain by protein kinase C: role of serine 24 phosphorylation. *Mol. Endocrinol.* **20**, 1838-1852. doi:10.1210/me.2005-0536

Okumura, T., Harada, K., Oue, K., Zhang, J., Asano, S., Hayashiuchi, M., Mizokami, A., Tanaka, H., Irifune, M., Kamata, N. et al. (2014). Phospholipase C-related catalytically inactive protein (PRIP) regulates lipolysis in adipose tissue by modulating the phosphorylation of hormone-sensitive lipase. *PLoS ONE* **9**, e100559. doi:10.1371/journal.pone.0100559

Oue, K., Zhang, J., Harada-Hada, K., Asano, S., Yamawaki, Y., Hayashiuchi, M., Furusho, H., Takata, T., Irifune, M., Hirata, M. et al. (2016). Phospholipase C-related catalytically inactive protein is a new modulator of thermogenesis promoted by β-adrenergic receptors in brown adipocytes. *J. Biol. Chem.* **291**, 4185-4196. doi:10.1074/jbc.M115.705723

Paz, K., Hemi, R., LeRoith, D., Karasik, A., Elhanany, E., Kanety, H. and Zick, Y. (1997). A molecular basis for insulin resistance. Elevated serine/threonine phosphorylation of IRS-1 and IRS-2 inhibits their binding to the juxtamembrane region of the insulin receptor and impairs their ability to undergo insulin-induced tyrosine phosphorylation. *J. Biol. Chem.* **272**, 29911-29918. doi:10.1074/jbc.272.47.29911

Ramos, R. R., Swanson, A. J. and Bass, J. (2007). Calreticulin and Hsp90 stabilize the human insulin receptor and promote its mobility in the endoplasmic reticulum. *Proc. Natl. Acad. Sci. USA* **104**, 10470-10475. doi:10.1073/pnas.0701114104

Romere, C., Duerrschmid, C., Bournat, J., Constable, P., Jain, M., Xia, F., Saha, P. K., Del Solar, M., Zhu, B., York, B. et al. (2016). Asprosin, a fasting-induced glucogenic protein hormone. *Cell* **165**, 566-579. doi:10.1016/j.cell.2016.02.063

Samuel, V. T. and Shulman, G. I. (2012). Mechanisms for insulin resistance: common threads and missing links. *Cell* **148**, 852-871. doi:10.1016/j.cell.2012.02.017

Shah, O. J., Wang, Z. and Hunter, T. (2004). Inappropriate activation of the TSC/Rheb/mTOR/S6K cassette induces IRS1/2 depletion, insulin resistance, and cell survival deficiencies. *Curr. Biol.* **14**, 1650-1656. doi:10.1016/j.cub.2004.08.026

Shearin, A. L., Monks, B. R., Seale, P. and Birnbaum, M. J. (2016). Lack of AKT in adipocytes causes severe lipodystrophy. *Mol. Metab.* **5**, 472-479. doi:10.1016/j.molmet.2016.05.006

Softic, S., Boucher, J., Solheim, M. H., Fujisaka, S., Haering, M.F., Homan, E. P., Winnay, J., Perez-Atayde, A.R. and Kahn, C.R. (2016). Lipodystrophy due to adipose tissue-specific insulin receptor knockout results in progressive NAFLD. Diabetes **65**, 2187–2200. doi:10.2337/db16-0213

Starks, R. D., Beyer, A. M., Guo, D. F., Boland, L., Zhang, Q., Sheffield, V. C. and Rahmouni, K. (2015). Regulation of insulin receptor trafficking by Bardet Biedl syndrome proteins. *PLoS Genet.* **11**, e1005311. doi:10.1371/journal.pgen.1005311

Su, X., Lodhi, I. J., Saltiel, A. R. and Stahl, P. D. (2006). Insulin-stimulated interaction between insulin receptor substrate 1 and p85α and activation of protein kinase B/Akt require Rab5. *J. Biol. Chem.* **281**, 27982-27990. doi:10.1074/jbc.M602873200

Sugiyama, G., Takeuchi, H., Nagano, K., Gao, J., Ohyama, Y., Mori, Y. and Hirata, M. (2012). Regulated interaction of protein phosphatase 1 and protein

phosphatase 2A with phospholipase C-related but catalytically inactive protein. *Biochemistry* **51**, 3394-3403. doi:10.1021/bi2018128

Sugiyama, G., Takeuchi, H., Kanematsu, T., Gao, J., Matsuda, M. and Hirata, M. (2013). Phospholipase C-related but catalytically inactive protein, PRIP as a scaffolding protein for phospho-regulation. *Adv. Biol. Regul.* **53**, 331-340. doi:10.1016/j.jbior.2013.07.001

Takeuchi, H., Kanematsu, T., Misumi, Y., Yaakob, H. B., Yagisawa, H., Ikehara, Y., Watanabe, Y., Tan, Z., Shears, S. B. and Hirata, M. (1996). Localization of a high-affinity inositol 1,4,5-trisphosphate/inositol 1,4,5,6-tetrakisphosphate binding domain to the pleckstrin homology module of a new 130 kDa protein: characterization of the determinants of structural specificity. *Biochem. J.* **318**, 561-568. doi:10.1042/bj3180561

Takeuchi, H., Oike, M., Paterson, H. F., Allen, V., Kanematsu, T., Ito, Y., Erneux, C., Katan, M. and Hirata, M. (2000). Inhibition of Ca^{2+}signalling by p130, a phospholipase-C-related catalytically inactive protein: critical role of the p130 pleckstrin homology domain. *Biochem. J.* **349**, 357-368. doi:10.1042/bj3490357

Terunuma, M., Jang, I.-S., Ha, S. H., Kittler, J. T., Kanematsu, T., Jovanovic, J. N., Nakayama, K. I., Akaike, N., Ryu, S. H., Moss, S. J. et al. (2004). $GABA_A$ receptor phospho-dependent modulation is regulated by phospholipase C-related inactive protein type 1, a novel protein phosphatase 1 anchoring protein. *J. Neurosci.* **24**, 7074-7084. doi:10.1523/JNEUROSCI.1323-04.2004

Tremblay, F., Brûlé, S., Hee Um, S., Li, Y., Masuda, K., Roden, M., Sun, X. J., Krebs, M., Polakiewicz, R. D., Thomas, G. et al. (2007). Identification of IRS-1 Ser-1101 as a target of S6K1 in nutrient- and obesity-induced insulin resistance. *Proc. Natl. Acad. Sci. USA* **104**, 14056-14061. doi:10.1073/pnas.0706517104

Tzatsos, A. (2009). Raptor binds the SAIN (Shc and IRS-1 NPXY binding) domain of insulin receptor substrate-1 (IRS-1) and regulates the phosphorylation of IRS-1 at Ser-636/639 by mTOR. *J. Biol. Chem.* **284**, 22525-22534. doi:10.1074/jbc.M109.027748

Tzatsos, A. and Kandror, K. V. (2006). Nutrients suppress phosphatidylinositol 3-kinase/Akt signaling via raptor-dependent mTOR-mediated insulin receptor substrate 1 phosphorylation. *Mol. Cell. Biol.* **26**, 63-76. doi:10.1128/MCB.26.1.63-76.2006

van Weert, A. W. M., Geuze, H. J., Groothuis, B. and Stoorvogel, W. (2000). Primaquine interferes with membrane recycling from endosomes to the plasma membrane through a direct interaction with endosomes which does not involve neutralisation of endosomal pH nor osmotic swelling of endosomes. *Eur. J. Cell Biol.* **79**, 394-399. doi:10.1078/0171-9335-00062

Yamawaki, Y., Shirawachi, S., Mizokami, A., Nozaki, K., Ito, H., Asano, S., Oue, K., Aizawa, H., Yamawaki, S., Hirata, M. et al. (2019). Phospholipase C-related catalytically inactive protein regulates lipopolysaccharide-induced hypothalamic inflammation-mediated anorexia in mice. *Neurochem. Int.* **131**, 104563. doi:10.1016/j.neuint.2019.104563

Yoneyama, Y., Inamitsu, T., Chida, K., Iemura, S.-I., Netsume, T., Maeda, T., Hakuno, F. and Takahashi, S.-I. (2018a). Serine phosphorylation by mTORC1 promotes IRS-1 degradation through SCFβ-TRCP E3 ubiquitin ligase. *iScience* **5**, 1-18. doi:10.1016/j.isci.2018.06.006

Yoneyama, Y., Lanzerstorfer, P., Niwa, H., Umehara, T., Shibano, T., Yokoyama, S., Chida, K., Weghuber, J., Hakuno, F. and Takahashi, S.-I. (2018b). IRS-1 acts as an endocytic regulator of IGF-I receptor to facilitate sustained IGF signaling. *eLife* **7**, e32893. doi:10.7554/eLife.32893

Yoshimura, K., Takeuchi, H., Sato, O., Hidaka, K., Doira, N., Terunuma, M., Harada, K., Ogawa, Y., Ito, Y., Kanematsu, T. et al. (2001). Interaction of p130 with, and consequent inhibition of, the catalytic subunit of protein phosphatase 1α. *J. Biol. Chem.* **276**, 17908-17913. doi:10.1074/jbc.M009677200

Zerial, M. and McBride, H. (2001). Rab proteins as membrane organizers. *Nat. Rev. Mol. Cell Biol.* **2**, 107-117. doi:10.1038/35052055

Zhang, J., Gao, Z., Yin, J. and Quon, M. J. and Ye, J. (2008). S6K directly phosphorylates IRS-1 on Ser-270 to promote insulin resistance in response to TNF-α signaling through IKK2. *J. Biol. Chem.* **283**, 35375-35382. doi:10.1074/jbc.M806480200

Zhang, Z., Takeuchi, H., Gao, J., Wang, D. G., James, D. J., Martin, T. F. J. and Hirata, M. (2013). PRIP (Phospholipase C-related but Catalytically Inactive Protein) inhibits exocytosis by direct interactions with syntaxin-1 and SNAP-25 through its C2 domain. *J. Biol. Chem.* **288**, 7769-7780. doi:10.1074/jbc.M112.419317

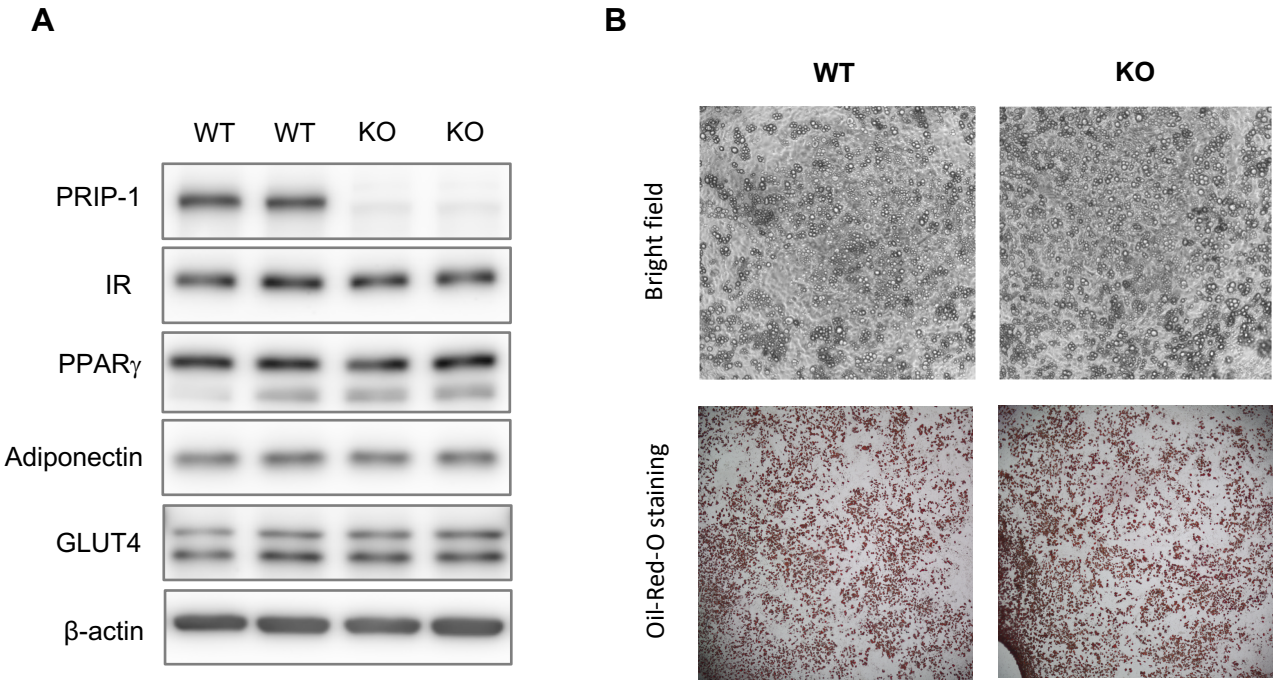

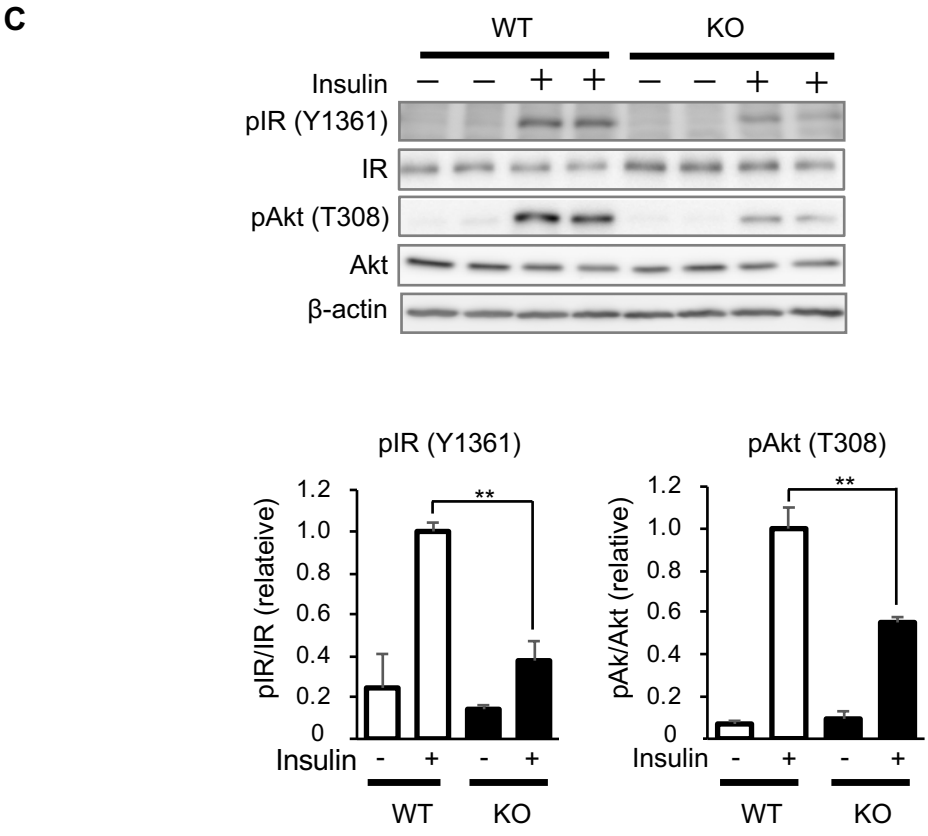

Fig. S1. (A) MEF cells isolated from WT and PRIP-KO mice were differentiated to adipocytes. The cell lysates were analyzed with SDS-PAGE and western blotting using the indicated antibodies. Representative blots are shown. **(B)** MEF cells isolated from WT and PRIP-KO mice were differentiated to adipocytes and subjected to Oil-Red-O staining. Representative mircoscopic images taken under bright field were shown. **(C)** Perigonadal white adipose tissue (pgWAT) were isolated from WT and PRIP-KO mice. The pgWAT were cut into small pieces and cultured in Medium 199 (free of serum) for 16 h, followed by stimulation with 5 nM Insulin for 15 min. The tissue lysates were prepared and 10 μg of proteins from each sample were loaded onto SDS-PAGE and analyzed by western blotting using indicated antibodies. Representative blots, as well as quantitative data are shown in the graph. Data are means ± SEM from four independent experiments. $^{**}P < 0.01$, *versus* the corresponding WT value.

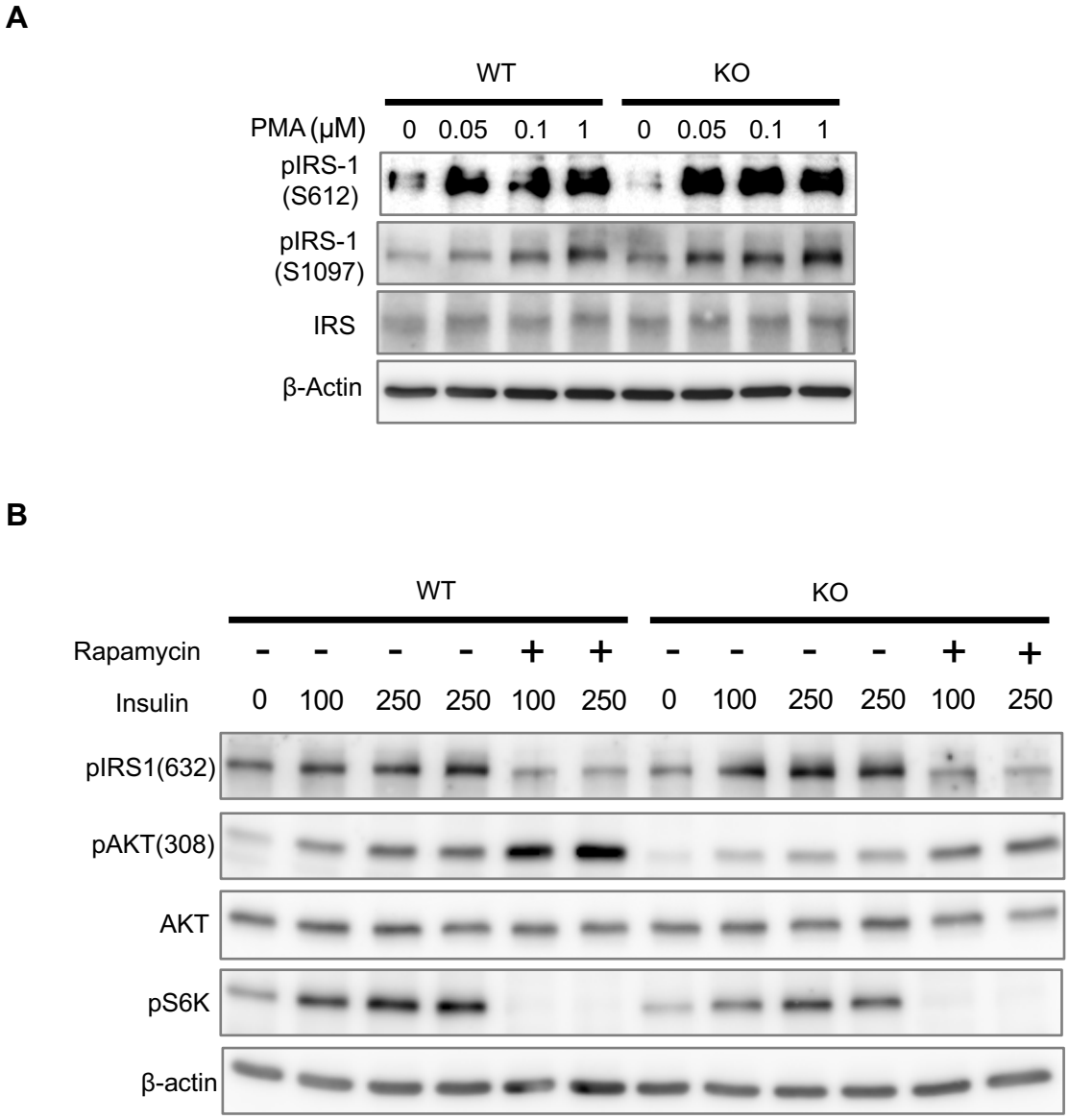

Fig. S2. (A) MEF cells isolated from WT and PRIP-KO mice were seeded on 12-well plate at $8x10^4$ cells/well and cultured for 24 h. After serum-starvation for 3 h, cells were stimulated with PMA at the indicated concentration for 30 min. **(B)** After serum starvation for 14 h and pretreatment with or without rapamycin (200 nM) for 1h, MEF cells on 12-well plate were stimulated with insulin at the indicated concentration for 30 min. The cell lysates were analyzed with SDS-PAGE and western blotting using the indicated antibodies. Representative blots are shown.

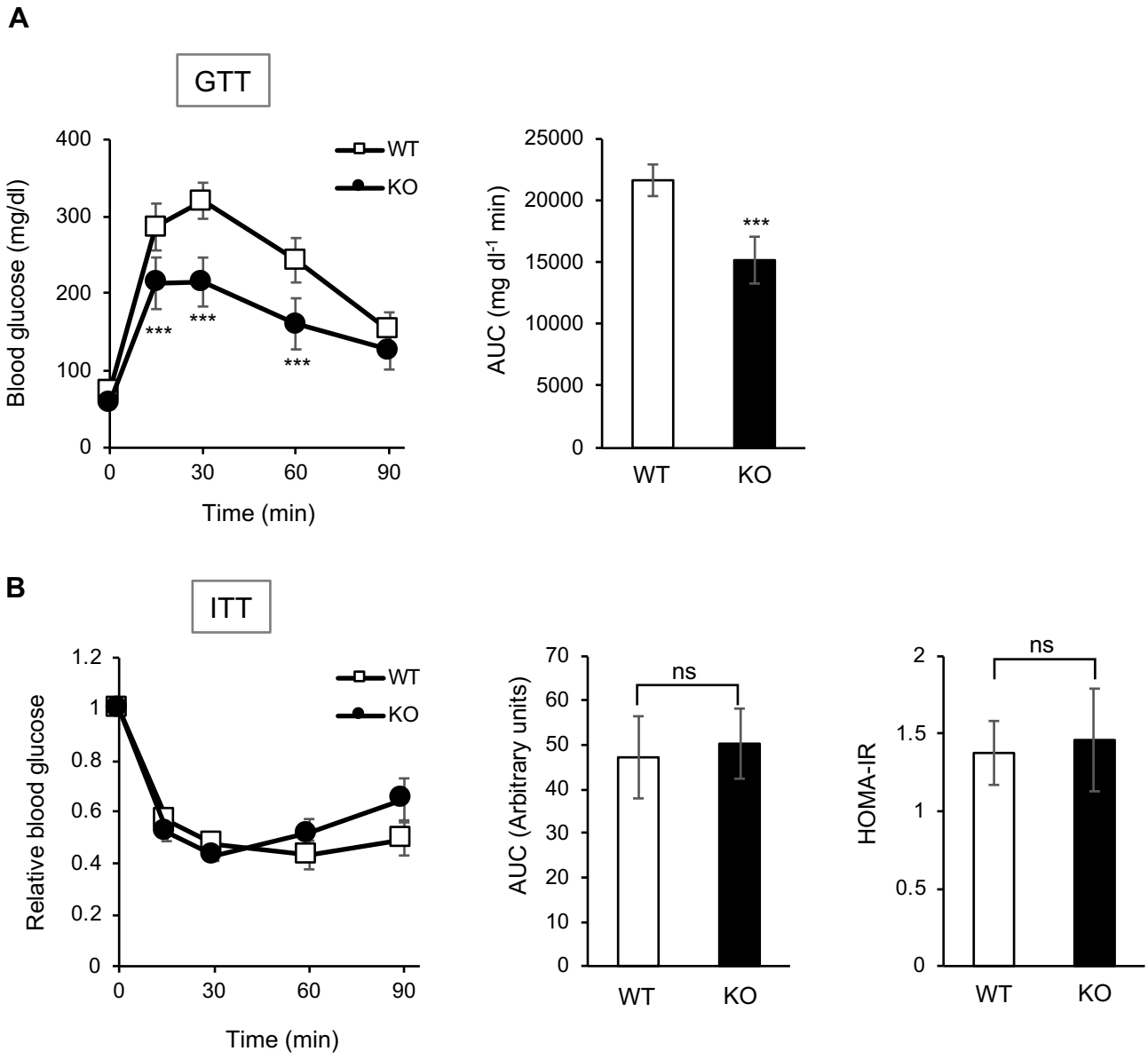

Fig. S3. (A) WT and PRIP-KO mice were subjected to an intraperitoneal glucose tolerance test at 10 weeks of age. The area under the curve (AUC) is shown on the right. The data represents means ± SD for 8 to 10 mice per group. ***p<0.0001 vs. the corresponding value for WT mice. Two-way ANOVA followed by Tukey's HSD for GTT, Student's t test for AUC. **(B)** WT and PRIP-KO mice were subjected to an intraperitoneal insulin tolerance test at 11 weeks of age. Graph on the left shows the relative blood glucose levels, and the area under the curve (AUC) is shown on the right. The data represents means ± SD for 8 to 10 mice per group. HOMA-IR was calculated using online-based calculator on the Diabetes Trials Unit of the University of Oxford website (https://www.dtu.ox.ac.uk/homacalculator/).

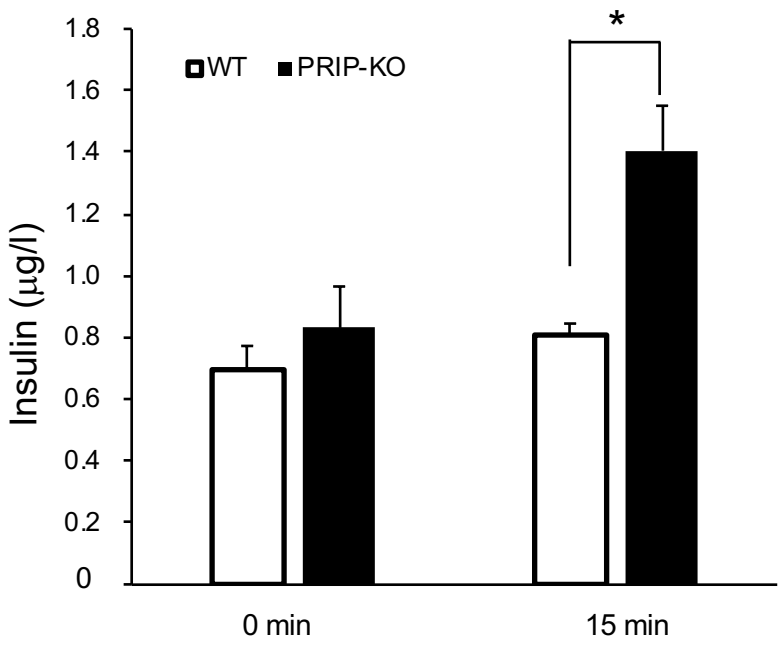

Fig. S4. Male mice of 12 weeks of age were fasted for 18 h and injected with 1g/kg glucose intraperitoneally. Serum insulin were collected at time 0 and 15 min after glucose injection. All data are means ± SEM (WT n=7, PRIP-KO n=8). WT, open bar and PRIP-KO, closed bar. *$P < 0.05$, *versus* WT value.